A Few Topics in micropump simulations

Chin-Tien Wu

Institute of Mathematical Modeling and Scientific Computation
Department of Applied mathematics
National Chiao-Tung University

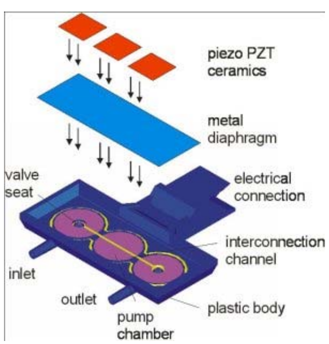

05/14/2010
台東大學綠色科技博覽會

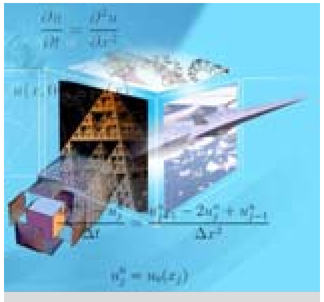

Motivations

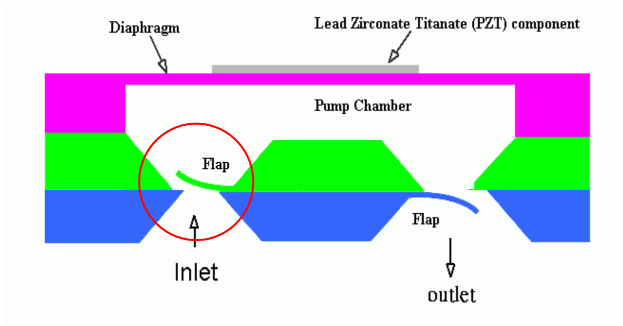

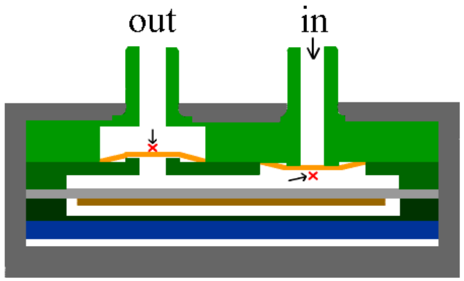

CurieJet Piezo MicroPump Animation

For designing a more reliable and efficient micro pump, it is important to understand:

(1) How the fluid interacts with the solid structure?
(2) How the composite membrane (a diaphragm coated with PZT ceramics) deform?
(3) Can we have a good frequency control on the diaphragm vibration such that the flux through the pump can be maximized?
(4) Can we detect or predict impurity of the PZT membrane to prevent possible malfunction of the pump?

we hope that numerical simulations can help in answering these questions

- (1) and (2) involve computational mechanics (including fluids and structures), solving PDEs with interfaces and solving PDEs on evolution surface.

- (3) and (4) involve solving polynomial eigenvalue problems especially for seeking resonance modes.

- For crack or intrusion detection in (4), one needs to solve inverse problems. For fracture and crack detection, singular solutions need to be computed.

Outline

- Incompressible Fluid simulations
- Nonlinear elasticity
- Piezoelectric material
- Potential problem on surfaces
- Interface problems
- Immersed finite element method for interface problems
- Intrusion detection problems
- conclusion

Incompressible fluid solver

$$\frac{\partial u}{\partial t} + u \nabla u - v \Delta u + \nabla p = 0 \quad \text{in } \Omega \times [0, T]$$

$$\nabla \cdot u = 0 \quad \text{in } \Omega \times [0, T],$$

$$u(x,t) = g(x,t) \quad \text{on } \partial\Omega \times [0, \mathrm{T}]$$

$$\mathrm{u}(\mathrm{x}, 0) = \mathrm{u}_0(x) \quad \text{in } \Omega$$

Time discretization (CN)

$$\frac{u^{n+1} - u^n}{\Delta t} - v \Delta u^{n+\theta} + u^* \nabla u^{n+\theta} + \nabla p^{n+\theta} = 0$$

$$\nabla \cdot u^{n+\theta} = 0 \text{ and } u^{n+\theta} = g \text{ on } \partial\Omega$$

Reynold’s number:

Space discretization

$$B_\delta \left\langle \left(u^{n+1}, p\right), (v, q) \right\rangle = \left(\frac{u^{n+1} - u^n}{\Delta t} - \varepsilon \Delta u^{n+\theta} + (u^* \cdot \nabla) u^{n+\theta} + \nabla p^{n+\theta}, v \right) +$$

$$\sum_T \left(\frac{u^{n+1} - u^n}{\Delta t} + (u^* \cdot \nabla) u^{n+\theta} + \nabla p^{n+\theta}, \tau_T \left[\left(u^* \cdot \nabla \right) v - \nabla q \right] \right) -$$

$$\sum_T \left(\nabla \cdot u^{n+\theta}, q - \delta_T \nabla \cdot v \right) = (f, v) + \sum_T \left(f, \tau_T \left[\left(u^* \cdot \nabla \right) v - \nabla q \right] \right)$$

flow passing around a cylinder

Re=20

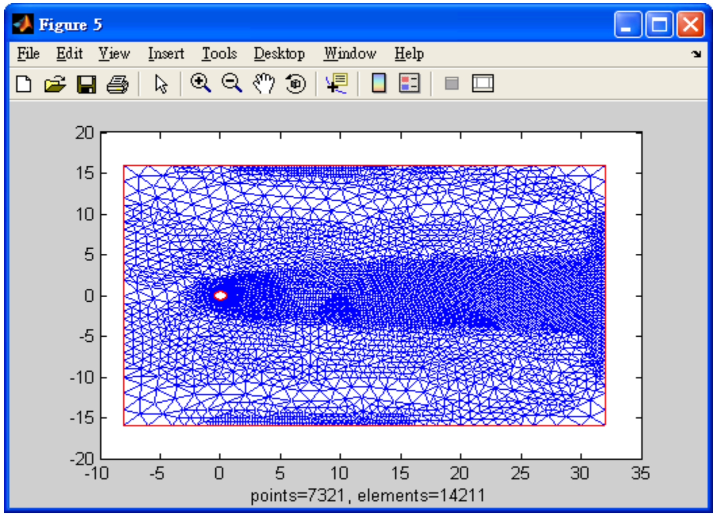

Re=200

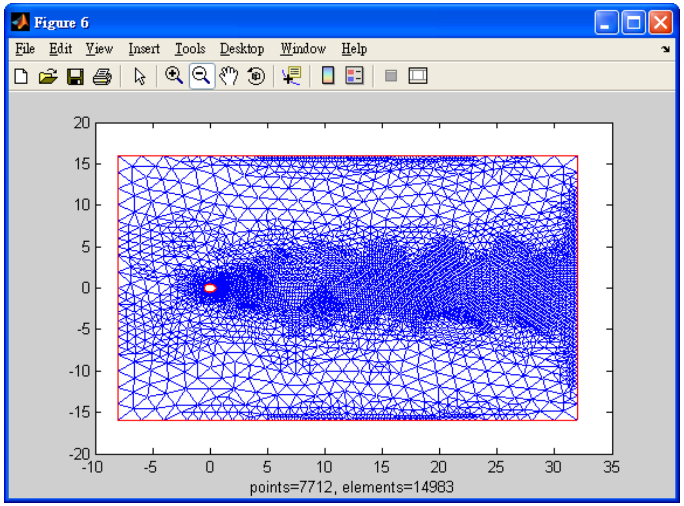

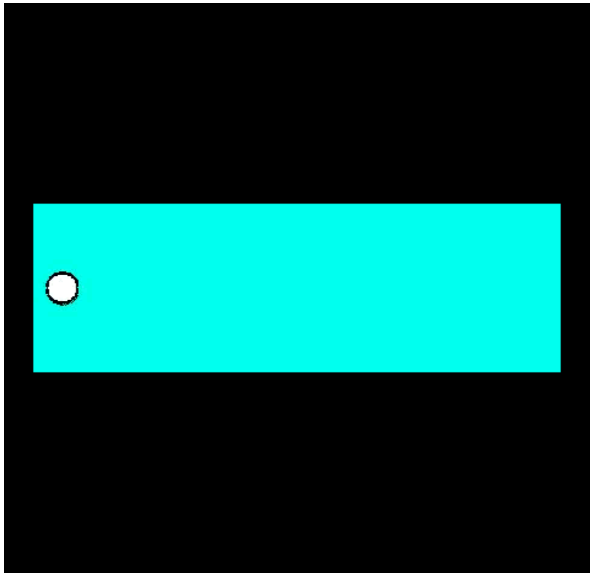

(B) Accuracy is achieved:

In the following, C_D=drag coefficient= $\dfrac{2F_d}{\rho U_\infty^2 L}$ C_L= lift coefficient= $\dfrac{2F_l}{\rho U_\infty^2 L}$

ST= Strouhal number= $\dfrac{freq * L}{\nu}$

Re	20		50		100		200	
C_D	2.11	2.22[1] 2.19[2]	1.46	1.41[1] 1.38[3]	1.38 ± 0.01	1.24[1] 1.35±0.012[4]	1.38 0.05	1.16[1] 1.31±0.049[4]
C_L	-	-	-	-	0.35	0.339[4]	0.7	0.69[4]
ST	-	-	0.125	0.12~0.13[1] 0.139[3]	0.167	0.167[1] 0.164[4]	0.2	0.19[4]

(1) for Re=100 and Re=200 are obtained experimentally by Clift and Reshko respectively.
(2) is computed on a 640x320 grid by Donna Calhoun, Courant Institute of mathematics science, in 2002.
(3) is computed on a 267x147 grid by Saki and Biringen, Dept. of Areospace Engineering, Univ. of Colorado, in 1996.
(4) is computed on a 256x256 grid by Liu, Zheng and Sung in 1998.

Simulation of flow, Re=10^6, around the airfoil NACA0012 with 20^o angle of attack

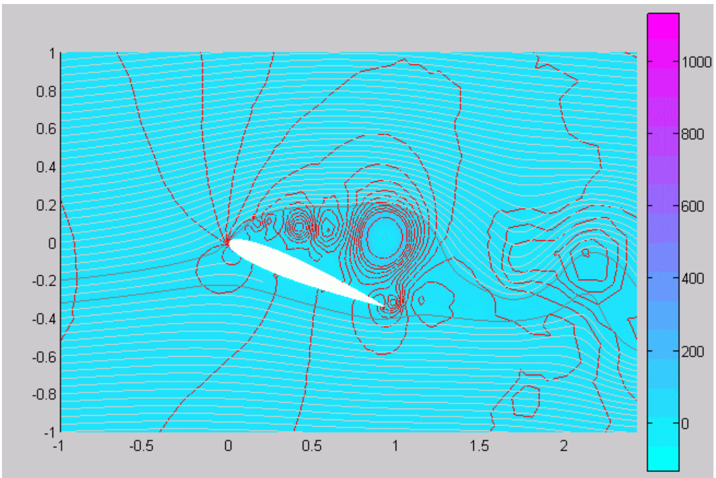

Chin-Tien's simulation on a grid with 4720 nodes

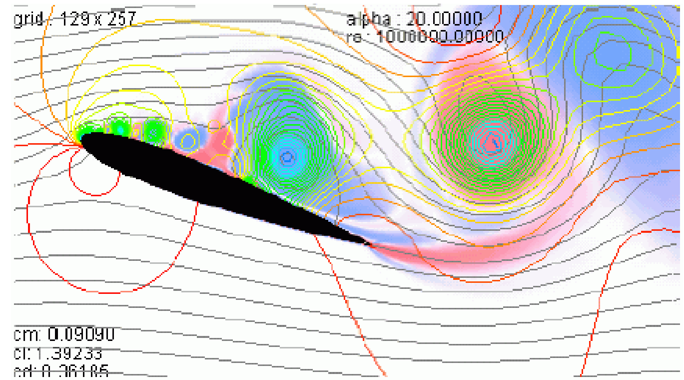

attack angle = 20 degrees

Figure 3 Instantaneous flow patterns in fine grid (128*256); stream lines, vorticity field, pressure contours

Kunio Kuwahara's simulation on a 128x256 grid (JSCFD 2000)

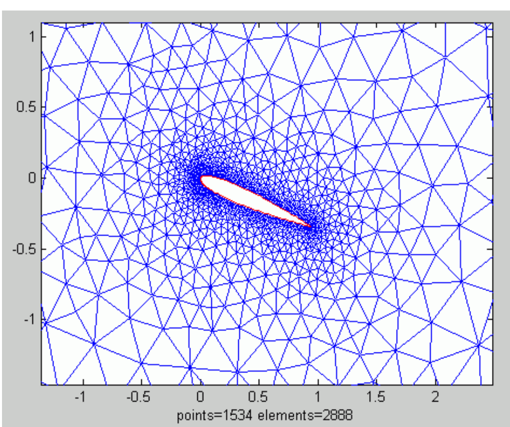

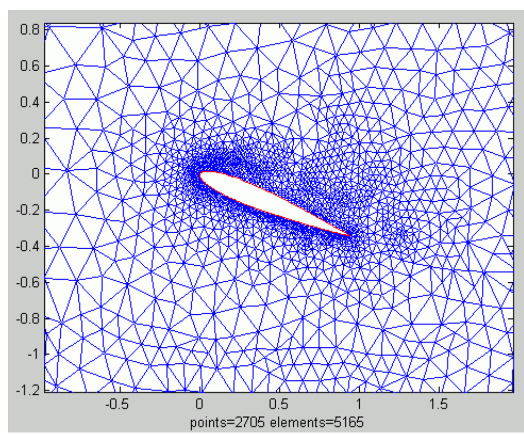

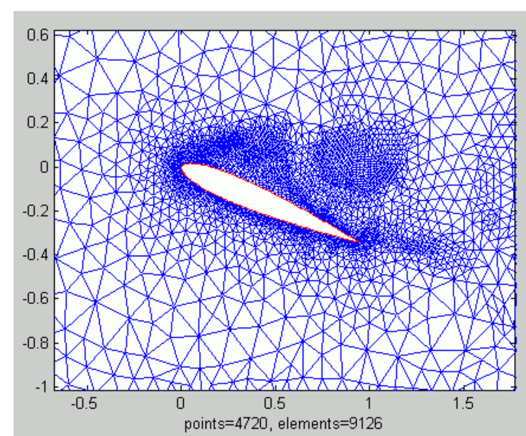

Cp of Naca0012 at 0° angle of attack with Re=3e+06

Fusen He and Tsung-Chow Su,
Journal of Wind Engineering and Industrial Aerodynamics, 1998, p.393-407.

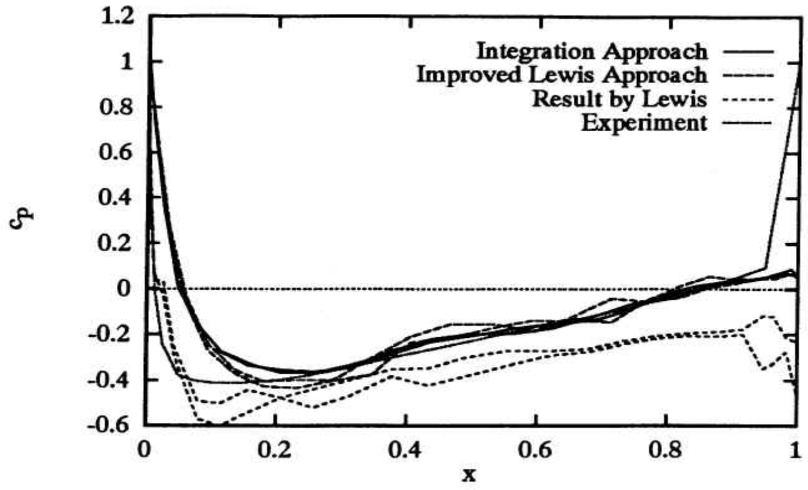

Chin Tien's simulation result

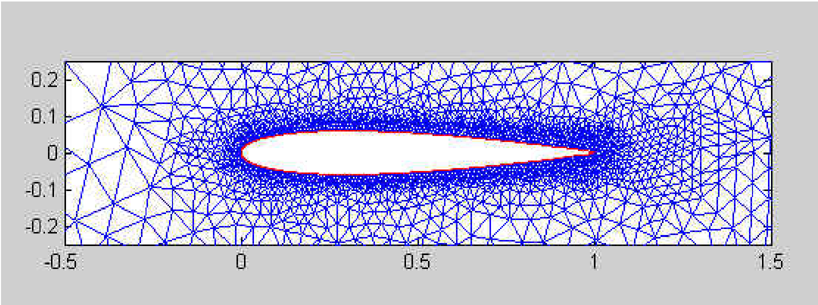

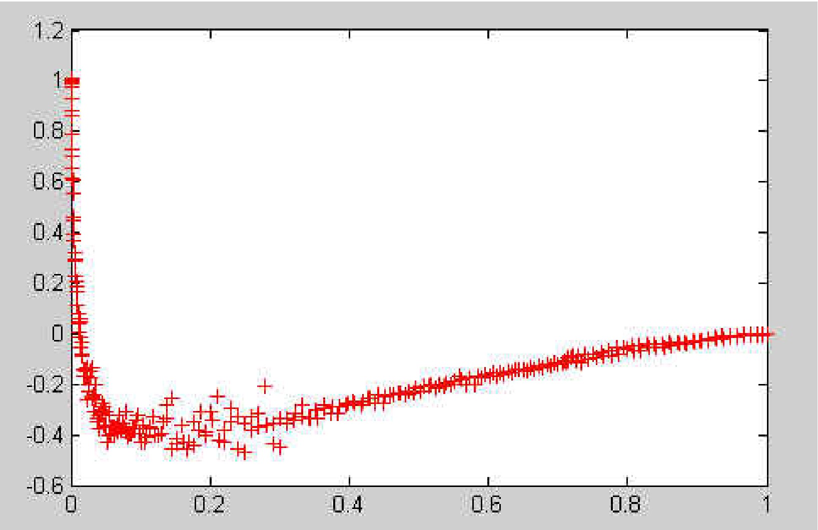

Number of points = 4984

400 time steps at △t=0.02 and
400 time steps at △t=0.01

Mathematical Modeling for large deformation of a elastic beam

Linear Euler-Bernoulli Beam

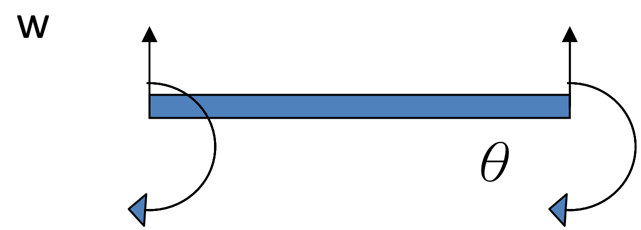

$$\varepsilon_{xx} = \frac{\partial u}{\partial x} = \frac{\partial u_0}{\partial x} + z\frac{\partial \theta_y}{\partial x} + y\frac{\partial \theta_z}{\partial x}$$

$$\delta_{xx} = E\varepsilon_{xx}$$

$$\delta\varepsilon_{xx} = \frac{\partial \delta u}{\partial x} = \frac{\partial \delta u_0}{\partial x} + z\frac{\partial \delta\theta_y}{\partial x} + y\frac{\partial \delta\theta_z}{\partial x}$$

$$\delta U = \int \delta\varepsilon_{xx}\sigma_{xx}dv$$

$$= \int_{X=0}^{L} EA\frac{\partial u_0}{\partial x}\frac{\partial \delta u_0}{\partial x}dx + \underbrace{\int_{X=0}^{L} EI_y\frac{\partial \theta_y}{\partial x}\frac{\partial \delta\theta_y}{\partial x}dx}_{\int EI_y \frac{\partial^2 \delta w}{\partial x^2}\frac{\partial^2 w}{\partial x^2}dx} + \int_{X=0}^{L} EI_z\frac{\partial \theta_z}{\partial x}\frac{\partial \delta\theta_z}{\partial x}dx$$

⇨ 4th order differential equation (Bi-harmonic equation)

Nonlinear Euler Beam

Geometry nonlinearity

$$E_{xx} = \frac{\partial u}{\partial x} + \frac{1}{2}((\frac{\partial u}{\partial x})^2 + (\frac{\partial v}{\partial x})^2 + (\frac{\partial w}{\partial x})^2)$$

$$= \frac{\partial}{\partial x}(u^{(i)} + \Delta u) + \frac{1}{2}\left[\left(\frac{\partial u^{(i)}}{\partial x} + \frac{\partial \Delta u}{\partial x}\right)^2 + \left(\frac{\partial v^{(i)}}{\partial x} + \frac{\partial \Delta v}{\partial x}\right)^2 + \left(\frac{\partial w^{(i)}}{\partial x} + \frac{\partial \Delta w}{\partial x}\right)^2\right]$$

$$= \frac{\partial u^{(i)}}{\partial x} + \frac{1}{2}\left[\left(\frac{\partial u^{(i)}}{\partial x}\right)^2 + \left(\frac{\partial v^{(i)}}{\partial x}\right)^2 + \left(\frac{\partial w^{(i)}}{\partial x}\right)^2\right]$$

$$+ \frac{\partial \Delta u}{\partial x} + \frac{\partial u^{(i)}}{\partial x}\frac{\partial \Delta u}{\partial x} + \frac{\partial v^{(i)}}{\partial x}\frac{\partial \Delta v}{\partial x} + \frac{\partial w^{(i)}}{\partial x}\frac{\partial \Delta w}{\partial x} + O\left((\Delta u)^2, (\Delta v)^2, (\Delta w)^2\right)$$

$$= E_{xx}^{(i)} + \Delta \varepsilon_{xx} + O\left((\Delta u)^2, (\Delta v)^2, (\Delta w)^2\right)$$

$$\delta E_{xx} = \frac{\partial \delta u}{\partial x} + \frac{\partial u^{(i)}}{\partial x}\frac{\partial \delta u}{\partial x} + \frac{\partial v^{(i)}}{\partial x}\frac{\partial \delta v}{\partial x} + \frac{\partial w^{(i)}}{\partial x}\frac{\partial \delta w}{\partial x}$$

$$+ \frac{\partial \Delta u}{\partial x}\frac{\partial \delta u}{\partial x} + \frac{\partial \Delta v}{\partial x}\frac{\partial \delta v}{\partial x} + \frac{\partial \Delta w}{\partial x}\frac{\partial \delta w}{\partial x}$$

$$= \delta \varepsilon_{xx} + \delta \eta_{xx}$$

$$\delta U = \int \left(\delta\varepsilon + \delta\eta\right)^{T}\left(S^{(i)} + \Delta S\right) dv$$

$$= \int \delta\varepsilon^{T} S^{(i)} + \int \delta\eta^{T} S^{(i)} + \int \delta\varepsilon^{T} \Delta S + \int \delta\eta^{T} \Delta S$$

$$= \underbrace{\int \delta\varepsilon^{T} C E^{(i)} + \int \delta\eta^{T} C E^{(i)}}_{\text{virtual work at i-th step}} + \underbrace{\int \delta\varepsilon^{T} C \Delta E + \int \delta\eta^{T} C \Delta E}_{\text{increment in Newton-Rapson}}$$

Full circle benchmark problem:

(1) bar length = 12, width and height of the cross section=1,

(2) end moment M=mf, here f varies from 0 to 2 and m=654761.9

(3) Young' s modulus = 3.0e+07, Poisson ratio=0,

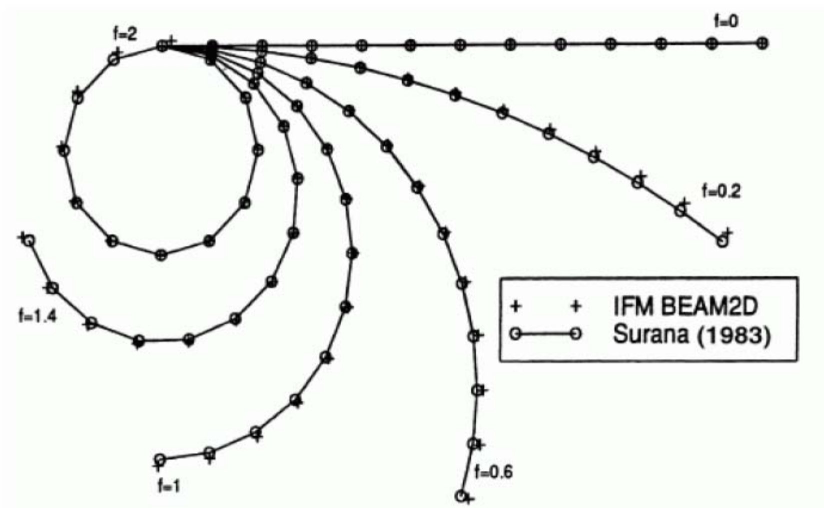

Figure 4. Deformed shapes of the cantilever beam with end moment.

Results from our codes

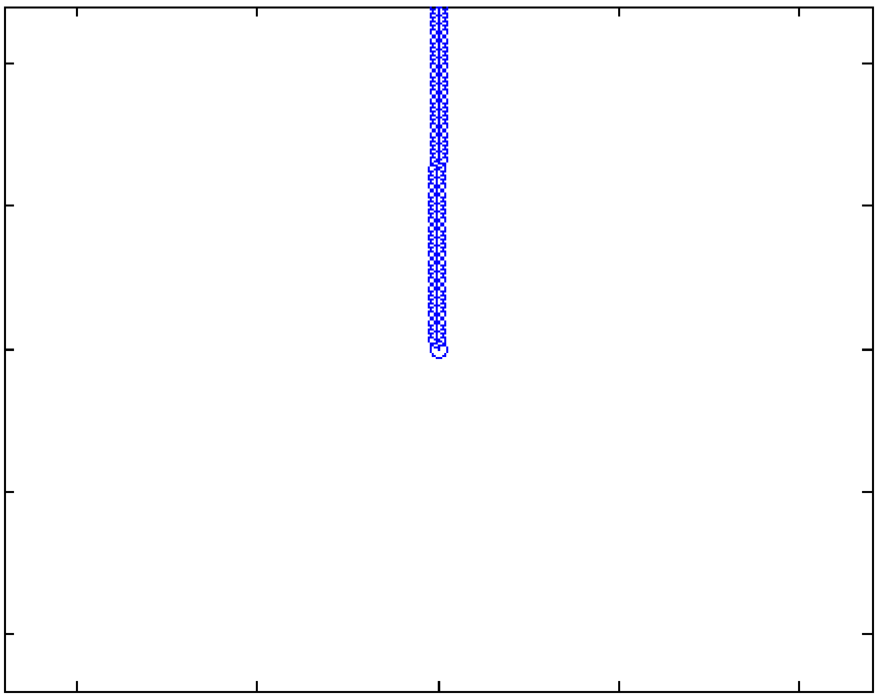

Original configuration

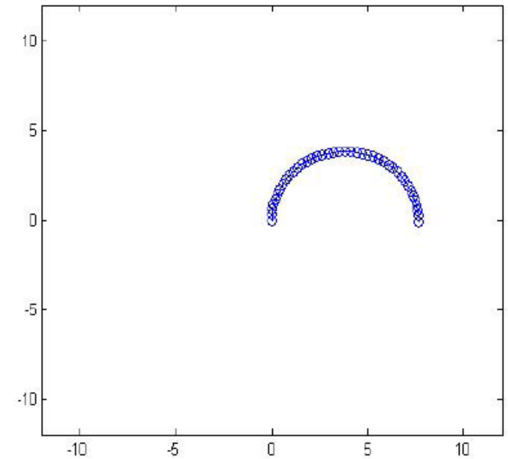

Configuration under 1M moment

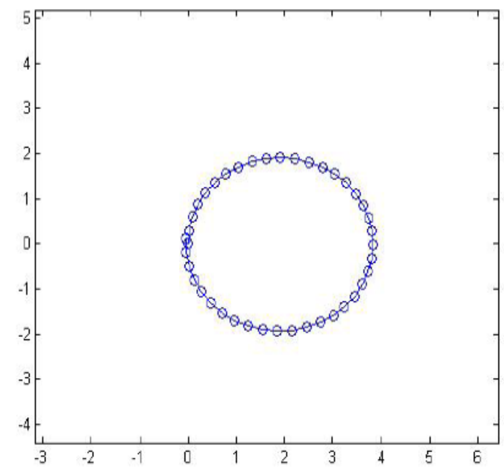

Configuration under 2M moment

4^{th} order bi-harmonic equation

Accuracy check for bi-harmonic solver (using BICZ element) :

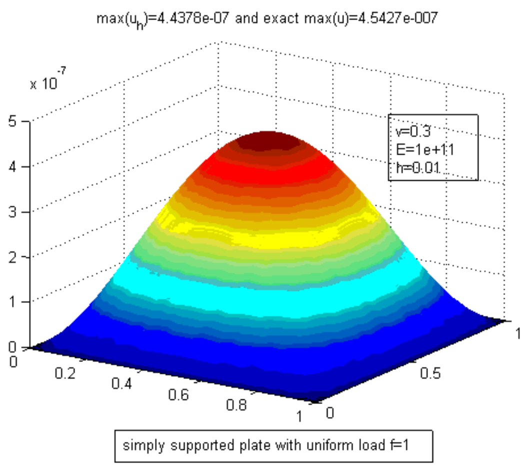

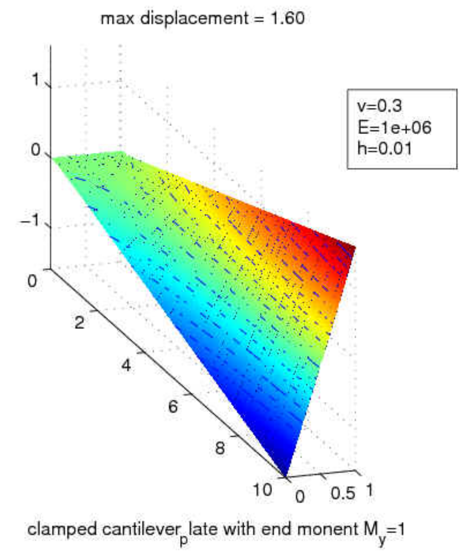

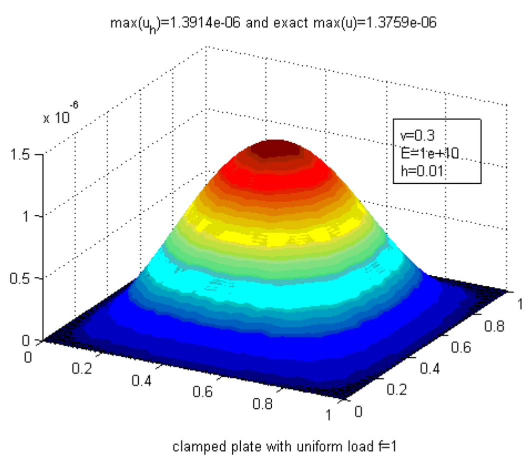

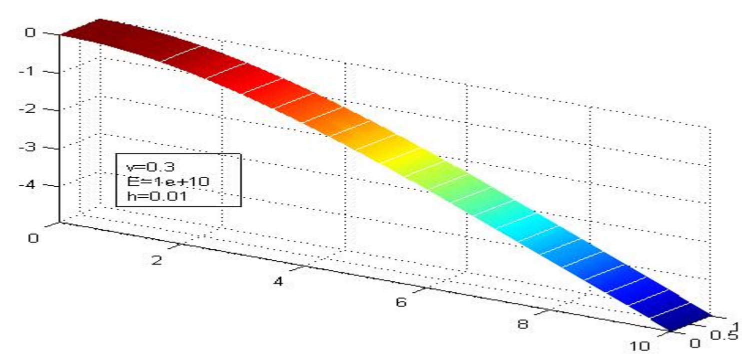

PZT simulation on saw filter

$$\sigma = C^{E}\varepsilon - e^{T}E$$

$$D = e\varepsilon + K^{\varepsilon}E$$

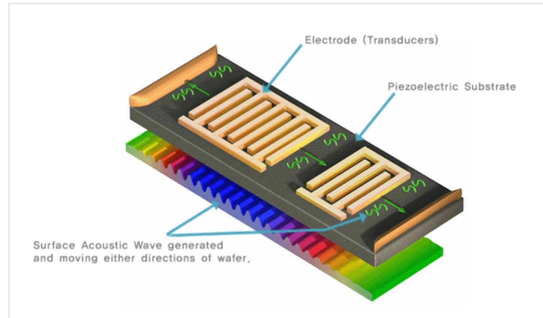

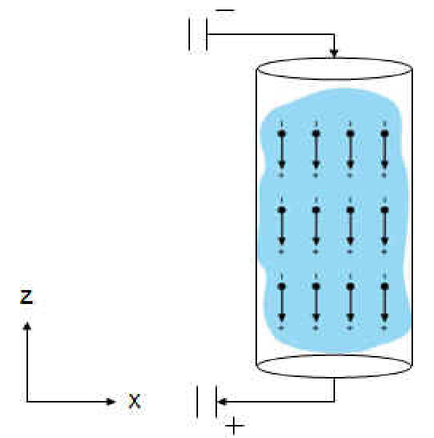

PZT during poling

$$C^{E} = \begin{bmatrix} c_{11} & c_{12} & c_{13} & 0 & 0 & 0 \\ c_{21} & c_{22} & c_{23} & 0 & 0 & 0 \\ c_{31} & c_{32} & c_{33} & 0 & 0 & 0 \\ 0 & 0 & 0 & c_{44} & 0 & 0 \\ 0 & 0 & 0 & 0 & c_{55} & 0 \\ 0 & 0 & 0 & 0 & 0 & \frac{1}{2}(c_{11}-c_{12}) \end{bmatrix}$$

$$K^{\varepsilon} = \begin{bmatrix} k_{11} & 0 & 0 \\ 0 & k_{22} & 0 \\ 0 & 0 & k_{33} \end{bmatrix}$$

$$e = \begin{bmatrix} 0 & 0 & 0 & 0 & e_{15} & 0 \\ 0 & 0 & 0 & e_{15} & 0 & 0 \\ e_{31} & e_{31} & e_{13} & 0 & 0 & 0 \end{bmatrix}$$

where σ and ε are the stress and strain tensors respectively, C^{E}, K^{ε} and e are the elasticity constant, dielectric constant and piezoelectric constant matrices measured at constant strain and constant temperature, D is the electric displacement and E is the electric field.

The unit cell problem

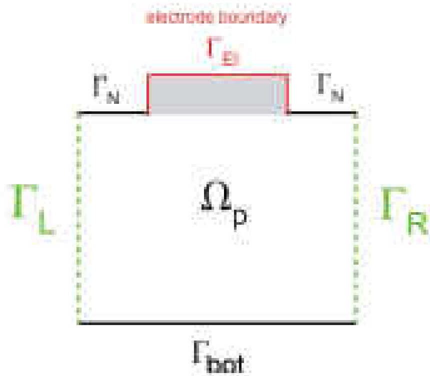

$$\begin{aligned}
-\operatorname{div}(c\,\tfrac{1}{2}((\nabla u)^T + \nabla u) + e^T\,\nabla\Phi) &= \omega^2 \rho u \text{ in } \Omega_P \\
-\operatorname{div}(e\,\tfrac{1}{2}((\nabla u)^T + \nabla u) - \epsilon\,\Phi) &= 0 \text{ in } \Omega_P \\
T.n = 0, D.n &= 0 \text{ on } \Gamma_N \\
\Phi &= 0 \text{ on } \Gamma_{El}
\end{aligned}$$

Quasi-periodic boundary conditions on Γ_L, Γ_R

$$\boxed{\begin{aligned}
\tilde{u}(p, x_2) &= \gamma\,\tilde{u}(0, x_2) \\
\frac{\partial \tilde{u}}{\partial N_r}(p, x_2) &= -\gamma \frac{\partial \tilde{u}}{\partial N_l}(0, x_2)
\end{aligned} \quad \text{with } \tilde{u} = (u_1, u_2, u_3, \Phi)}$$

with propagation parameter $\gamma := e^{(\alpha + i\beta)p}$.

The frequency-dependent eigenvalue problem

For given parameters ω^2 search for $(\gamma, (u, \lambda)^T)$ such that

$$
\begin{array}{rcll}
\overbrace{a(u,v) + i\,\omega\, c(u,v) - \omega^2 m(u,v)}^{k(\omega)(u,v)} \;+\; < (tr_l^* - \gamma tr_r^*)\lambda, v > & = & 0 & \forall\, v \in \left[H^1(\Omega)\right]^4 \\
< (tr_r - \gamma tr_l)u, \mu > & = & 0 & \forall\, \mu \in \left[H^{-0.5}(\Gamma)\right]^4
\end{array}
$$

The FE-discretiszed problem is of the form

$$
\begin{pmatrix} \overline{K}(\omega) & Tr_l^T \\ Tr_r & 0 \end{pmatrix} \begin{pmatrix} u_h \\ \lambda_h \end{pmatrix} = \gamma \begin{pmatrix} 0 & Tr_r^T \\ Tr_l & 0 \end{pmatrix} \begin{pmatrix} u_h \\ \lambda_h \end{pmatrix}
$$

with $\overline{K} := K + i\omega C - \omega^2 M$ complex-symmetric and indefinite (of saddle point structure).

Simulation results from 36^{o} YX-Cut $LiTaO_3$

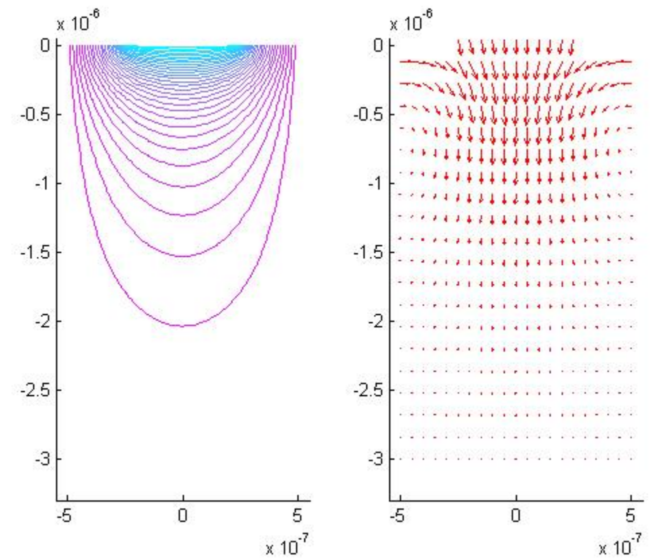

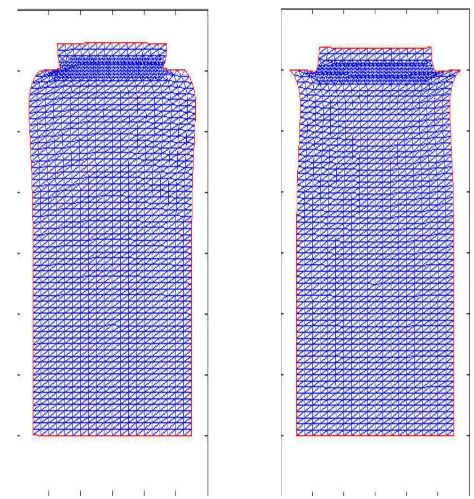

Potential=100 Potential=-100

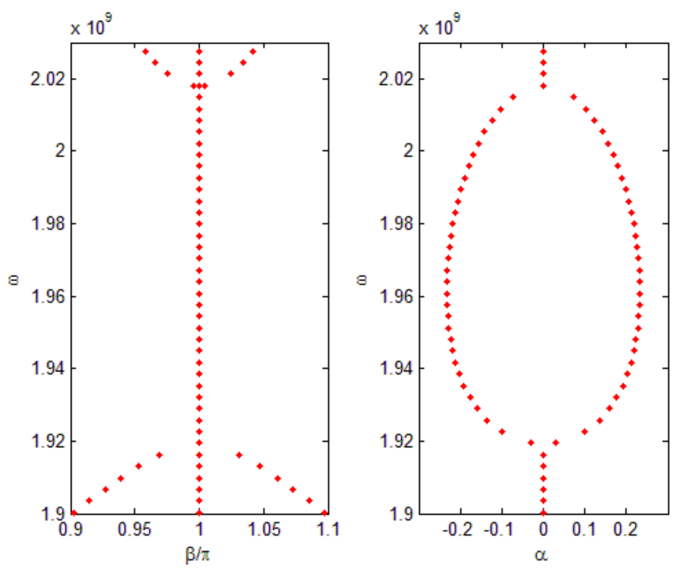

Simulation from our code

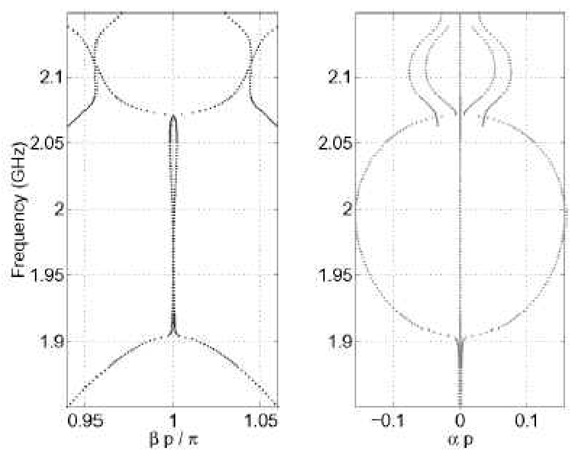

Fig. 14. Simulated propagation constant β and decay constant α.

Result from Hofer and zaglmayer, IEEE Transaction on ultrasonic, Ferroelectric and Frequency control, 2006.

SAW in fluid transfer

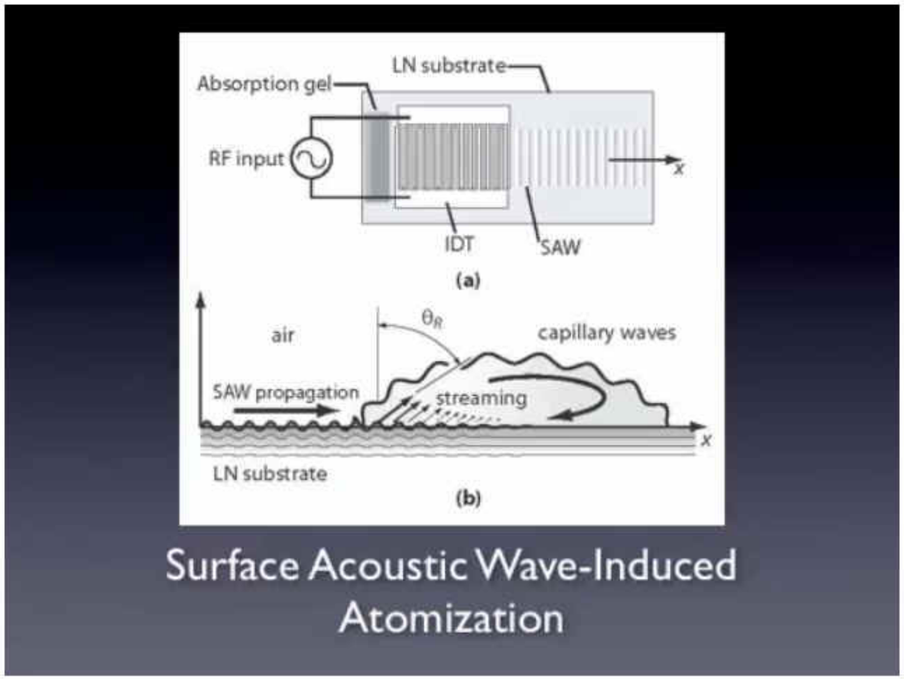

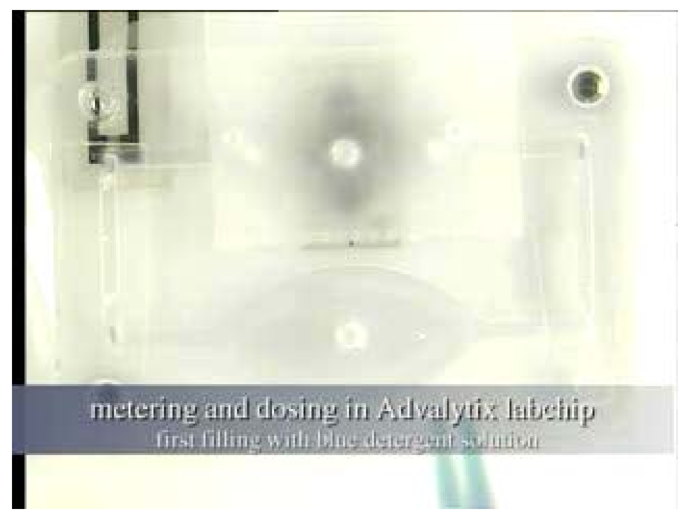

Solving Laplace on evolution surface

$$\frac{\mathrm{d}}{\mathrm{d}t}\int_{\mathscr{M}(t)} u = -\int_{\partial\mathscr{M}(t)} q\cdot\mu, \quad \Longrightarrow \quad \dot{u} + u\nabla_\Gamma\cdot v + \nabla_\Gamma\cdot q = 0.$$

FEM accuracy check for surface laplacian: u(x,y)=x*y

mesh points	max err	relative L2 err
162	0.03164	0.0597
642	0.00885	0.0154
2562	0.0024	0.0038

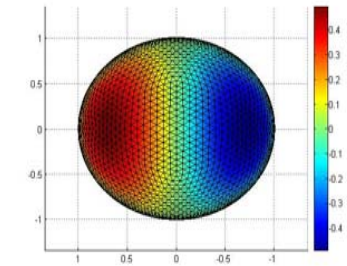

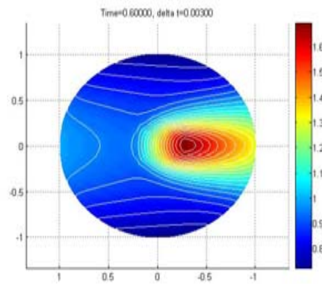

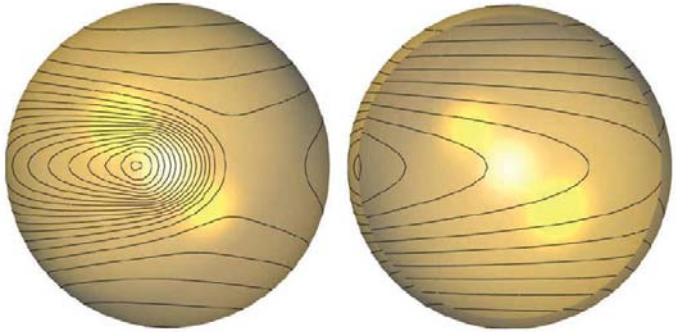

FIG. 6. Level lines of the stationary solution of Example 7.5. Front side of the sphere (left) and backside (right).

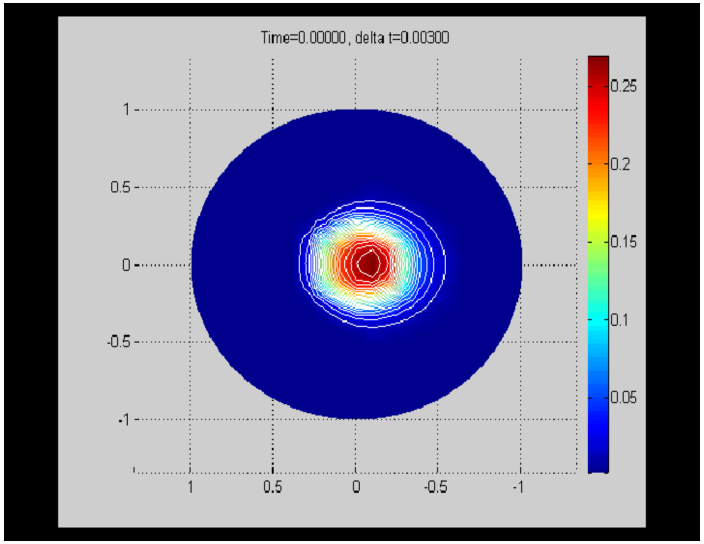

Numerical results from G. Dziuk and C. M. Elliott,
Finite elements on evolving surfaces, IMA J. Numer. Anal.
2007

Interface problems

- 2nd order elliptic interface problems: heat diffusion, electric potential and plane elasticity for composite materials

$$\nabla \cdot \sigma + F = 0 \qquad \text{in } \Omega^- \cup \Omega^+,$$
$$u = G \qquad \text{on } \partial\Omega.$$
$$\sigma = \alpha \nabla u$$

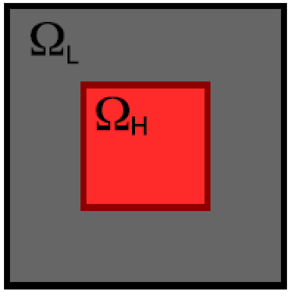

- 4th order elliptic interface problems: composite membrane bending

$$\begin{aligned} \nabla^2 \left(\alpha \nabla^2 u\right) &= f \qquad \text{in} \quad \Omega \subset \mathbb{R}^2, \\ u = \partial_n u &= 0 \qquad \text{on} \quad \partial\Omega. \end{aligned}$$

2nd coupled with 4th order interface problems:

- Structure-Structure interactions:

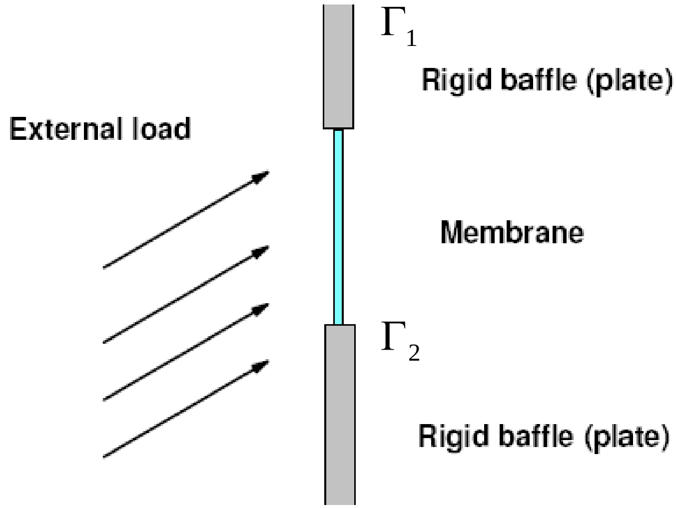

$$\begin{cases} -\Delta u_1 + \alpha u_1 = f & \text{in } \Omega_1 \\ u_1 = 0 & \text{on } \Gamma_1 \end{cases}$$

$$\begin{cases} \sigma^2 \Delta^2 u_2 - \Delta u_2 + \alpha u_2 = f & \text{in } \Omega_2, \\ u_2 = \partial u_2 / \partial n = 0 & \text{on } \Gamma_2, \end{cases}$$

Plate-membrane coupling: modeling the acoustic

characteristics of baffled membranes and the surrounding sound fields (sound insulation performance of building elements).

Paloa Gervasio, Homogeneous and heterogeneous domain decomposition methods for plate bending problems, Comput. Methods Appl. Mech. Engrg. 194 (2005) 4321–4343

Interface conditions

- 2^{nd} order elliptic interface problems

$$[u]_\Gamma = W,$$

$$[\sigma n]_\Gamma = Q,$$

- 4^{th} order elliptic interface problems

$$[u] = 0$$

$$[u_x] = [u_y] = 0$$

$$[\alpha \Delta u] = 0$$

$$\left[\alpha \frac{\partial}{\partial n} \Delta u\right] = 0$$

- 2^{nd} coupled with 4^{th} order interface problems:
    - Structure-Structure interactions:

$$u_2 - u_1 = g_1,$$

$$\sigma \Delta u_2 = g_2,$$

$$\mathbf{n} \cdot (-\nabla(\sigma \Delta u_2)) - T\mathbf{n} \cdot \nabla u_1 = g_3 \quad on \quad \Gamma.$$

Lopatinski–Shapiro conditions

Given an elliptic interface problem, the interface conditions will lead to a well-posed problem, if and only if, they satisfy the so called covering conditions or Lopatinski–Shapiro conditions

Definition

The system of interface operators $B_{i,j-1}(x;D)$, $i=1,2; j=1,...,m_1+m_2$ cover the pair of elliptic operators $P_1(x;D), P_2(x;D)$ at the interface Γ,if

$$d(x_0;\xi) = \det \begin{pmatrix} b^1_{11}(\xi) & b^1_{21}(\xi) & \dots & b^1_{m_1+m_2 1}(\xi) \\ \dots & \dots & \dots & \dots \\ b^1_{1m_1}(\xi) & b^1_{2m_1}(\xi) & \dots & b^1_{m_1+m_2 m_1}(\xi) \\ b^2_{11}(\xi) & b^2_{21}(\xi) & \dots & b^2_{m_1+m_2 1}(\xi) \\ \dots & \dots & \dots & \dots \\ b^2_{1m_1}(\xi) & b^2_{2m_1}(\xi) & \dots & b^2_{m_1+m_2 m_2}(\xi) \end{pmatrix} \neq 0$$

for any $x_0 \in \Gamma, \xi \neq 0$.

Igor Mozolevski and Endre Süli, Discontinuous Galerkin Method for interface problem of coupling different order elliptic equations, 5th European Finite Element Fair Marseille (France),17–19 May 2007

- Fluid-Structure interactions:

$$\rho^f\left(\frac{\partial}{\partial t}u^f + u^f\cdot\nabla u^f\right)+\nabla p^f = div\left(\sigma^f\right)+g_b^f$$

$$\nabla\cdot u^f = 0$$

$$u^f\Big|_{\Gamma_1} = u^s\Big|_{\Gamma_1},\ u^f\Big|_{\Gamma_2} = \left(\bar{u}^f_{mean}, 0\right),$$

$$here\ \sigma^f = -p^f I + \rho^f\varepsilon\left(\nabla u^f + \nabla u^{f^T}\right)$$

$$\rho^s\left(\frac{\partial}{\partial t}u^s + \left(\nabla u^s\right)u^s\right) = \nabla\cdot\sigma^s + g_b^s$$

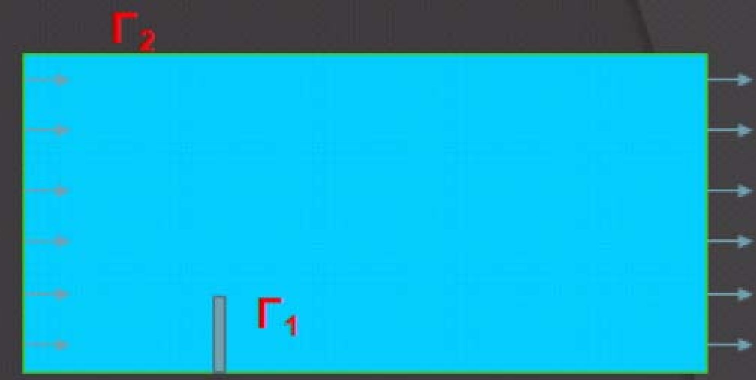

$$\sigma^s\cdot\vec{n} = \sigma^f\cdot\vec{n} \text{ and } u^s\Big|_{\Gamma_1} = u^f\Big|_{\Gamma_1}$$ Interface conditions

here σ^s is the Cauchy stress tensor defined as

$$\sigma^s = \frac{1}{\det(F)}F\left(\lambda^s\cdot tr(E)I + 2\mu^s E\right)F^T,$$

$$F = I + \nabla u^s \text{ and } \mathrm{E} = \frac{1}{2}\left(F^T F - I\right).$$

Moving mesh in FSI simulations

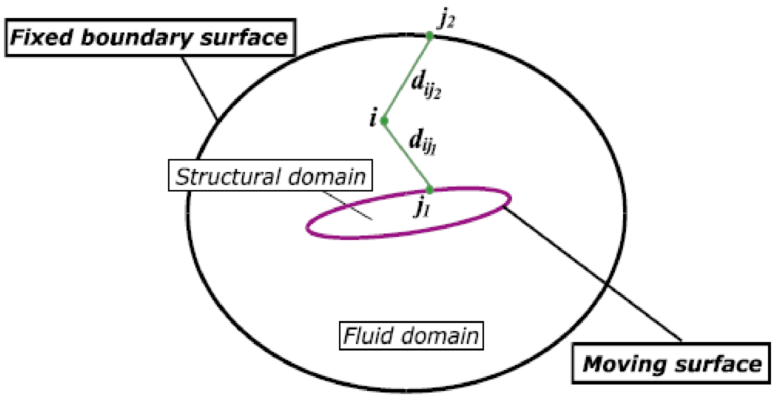

$$\mathbf{w}^i = \frac{\sum_{j=1}^{ns} a_{ij}\mathbf{w}^j}{\sum_{j=1}^{ns} a_{ij}} \qquad a_{ij} = \frac{1}{d_{ij}^4}$$

P.R.F. Teixeira and A.M. Awruch , Computers & Fluids, 34 (2005) 249–273 2005

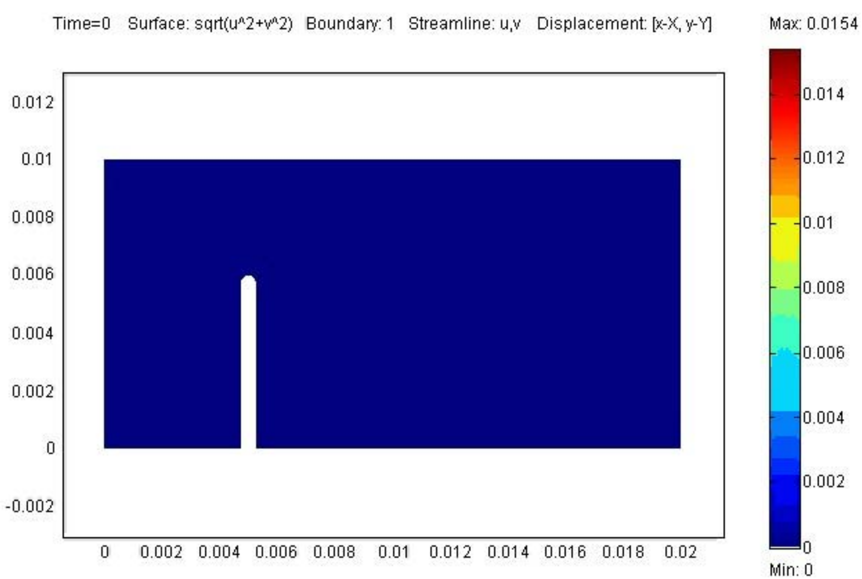

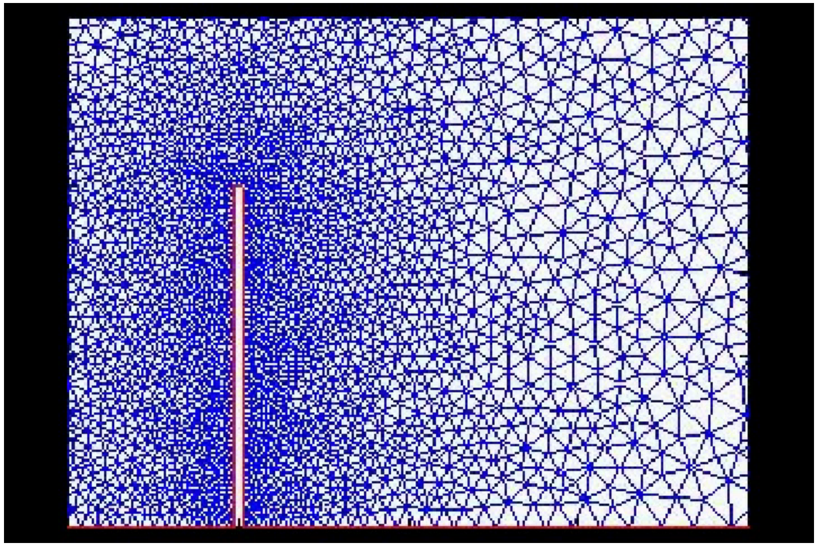

Simulation result from our code

What is troubling us?

- Accuracy on the interface degrades seriously as the jump ratio of the coefficient σ becomes large.

- Convergence rate of the linear solver such as multigrid iterative method decreases.

- For FSI dynamic simulation, moving mesh strategies are expansive and failure occurs sometimes due to improper time step size.

Toward to overcome the difficulties arising from interfaces

Immersed finite element method

In IFEM, the basis functions of the interface element are constructed to satisfy the interface conditions !

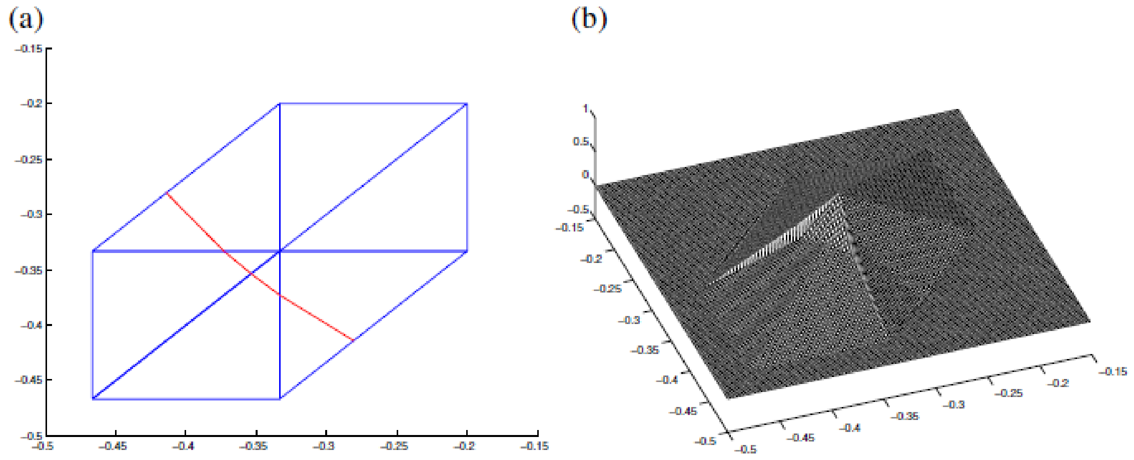

Fig. 2.2. (a): A standard domain of six triangles with an interface cutting through. (b): A global basis function on its support in the non-conforming immersed finite element space. The basis function has small jump across some edges

A simple 1-d 2nd order problem

$$(\beta u_x)_x = 12x^2, \qquad 0 \leqslant x \leqslant 1, \quad \beta = \begin{cases} \beta^- & \text{if } x < \alpha, \\ \beta^+ & \text{if } x > \alpha, \end{cases}$$

$$u(0) = 0, \qquad u(1) = 1/\beta^+ + \left(1/\beta^- - 1/\beta^+\right)\alpha^4.$$

$$u(x) = \begin{cases} x^4/\beta^- & \text{if } x < \alpha, \\ x^4/\beta^+ + \left(1/\beta^- - 1/\beta^+\right)\alpha^4 & \text{if } x > \alpha, \end{cases}$$

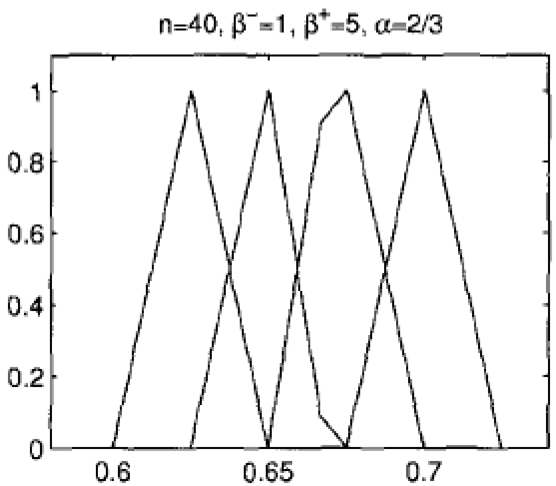

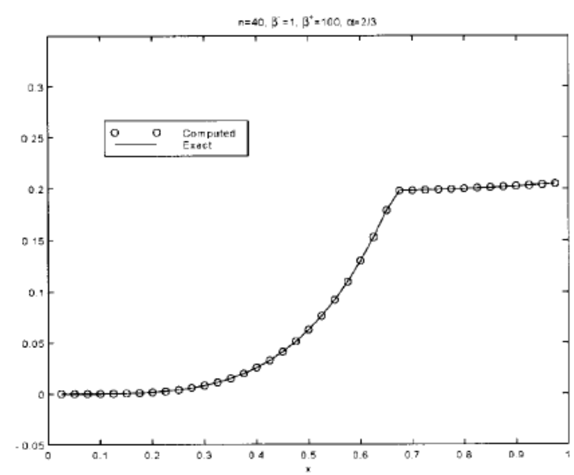

A simple 4th order problem

$$\Delta\left(\beta\Delta u\right)=24$$

$$u\left(0\right)=u'\left(0\right)=0;u\left(1\right)=\frac{1-2\alpha^2}{\beta^+}-\alpha^4\left(\frac{1}{\beta^-}-\frac{1}{\beta^+}\right),u'\left(1\right)=4\frac{\left(1-\alpha^2\right)}{\beta^+}$$

rigid connection interface conditions:

$$\left[u\right]_\alpha=0;\left[u'\right]_\alpha=0;\left[\beta u''\right]_\alpha=0;\left[\beta u'''\right]_\alpha=0;$$

Finite element basis:

$$N_{w1}=1-3s^2+2s^3$$
$$N_{\theta 1}=(-s+2s^2-s^3)h$$
$$N_{w2}=3s^2-2s^3$$
$$N_{\theta 2}=(s^2-s^3)h$$

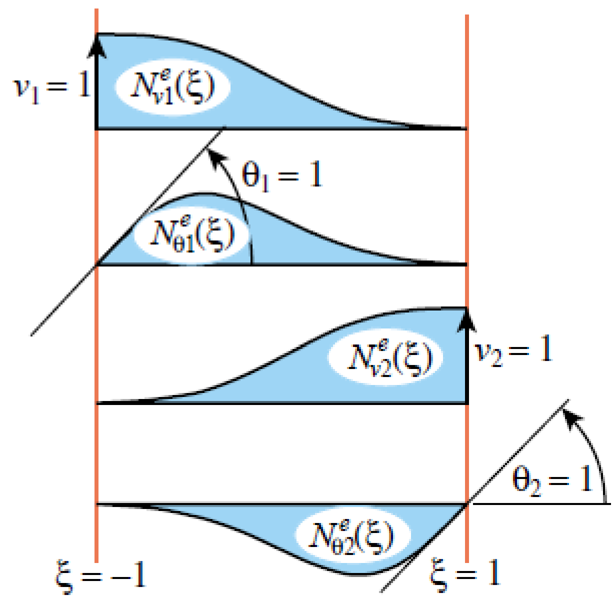

FIGURE 12.10. Cubic shape functions of plane beam element.

IFEM for bi-harmonic equations

Assume the basis functions of the interface elements are

$$\phi^{-}(x) = a_0 + a_1 x + a_2 x^2 + a_3 x^3$$

$$\phi^{+}(x) = b_0 + b_1 x + b_2 x^2 + b_3 x^3$$

Enforce the interface conditions and nodal continuity, to determine the coefficients, one simply need to solve the following linear system:

$$\begin{bmatrix} 1 & 0 & 0 & 0 & 0 & 0 & 0 & 0 \\ 0 & \frac{1}{h} & 0 & 0 & 0 & 0 & 0 & 0 \\ 0 & 0 & 0 & 0 & 1 & 1 & 1 & 1 \\ 0 & 0 & 0 & 0 & 0 & \frac{1}{h} & \frac{2}{h} & \frac{3}{h} \\ 1 & s & s^2 & s^3 & -1 & -s & -s^2 & -s^3 \\ 0 & \frac{1}{h} & \frac{2s}{h} & \frac{3s^2}{h} & 0 & -\frac{1}{h} & -\frac{2s}{h} & -\frac{3s^2}{h} \\ 0 & 0 & \frac{2\beta^-}{h^2} & \frac{6s\beta^-}{h^2} & 0 & 0 & -\frac{2\beta^+}{h^2} & -\frac{6s\beta^+}{h^2} \\ 0 & 0 & 0 & \frac{6\beta^-}{h^3} & 0 & 0 & 0 & -\frac{6\beta^-}{h^3} \end{bmatrix} \begin{bmatrix} a_0 \\ a_1 \\ a_2 \\ a_3 \\ b_0 \\ b_1 \\ b_2 \\ b_3 \end{bmatrix} = \begin{bmatrix} \phi_a \\ \phi_a' \\ \phi_b \\ \phi_b' \\ 0 \\ 0 \\ 0 \\ 0 \end{bmatrix}$$

Results from our code

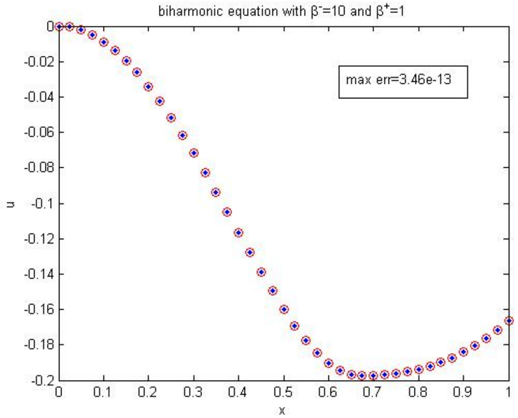

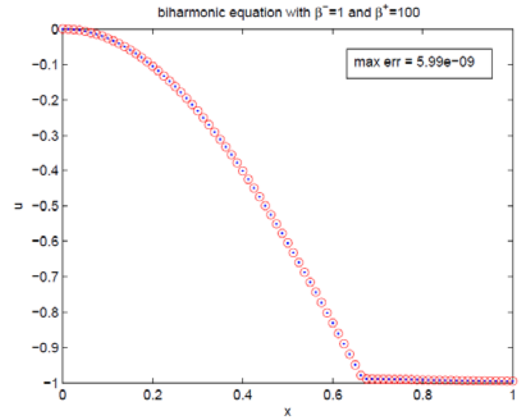

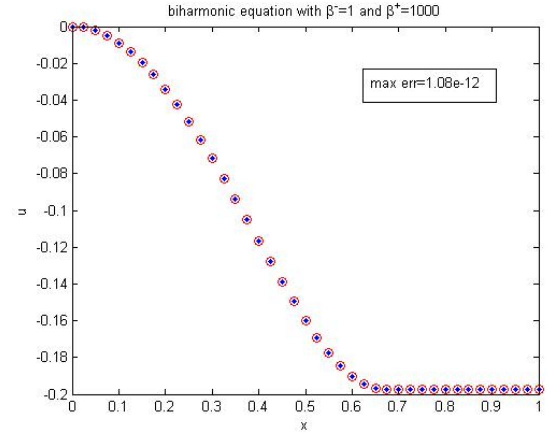

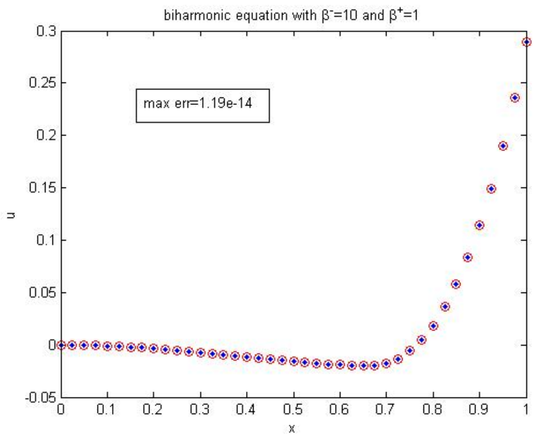

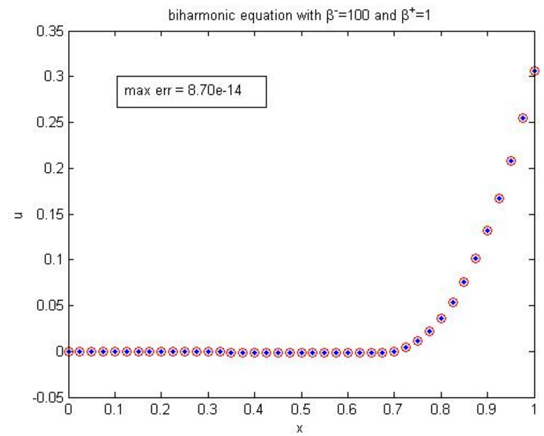

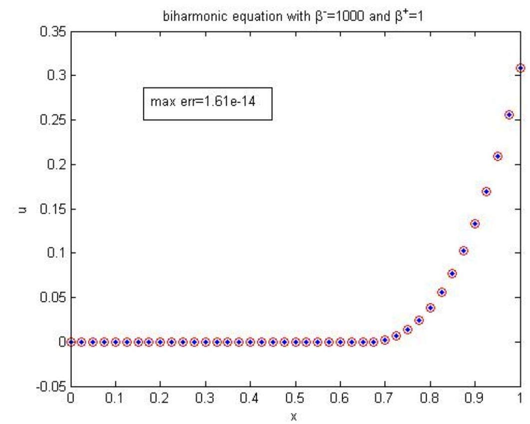

BVP for the beam equation

$$(\beta(x)u''(x))'' = f(x), x \in \Omega = (0,1)$$

$$u(0) = u'(0) = u(1) = u'(1) = 0$$

Consider a model interface problem with the exact solution:

$$u(x) = \begin{cases} a\cos(x) + b\sin(x), 0 < x < \alpha \\ ce^{x} + dx^{3} + 5, \alpha \leq x < 1 \end{cases}$$

in which the coefficients *a, b, c, d* are chosen so that u satisfies:

$$[u]_\alpha = [u']_\alpha = [\beta u'']_\alpha = [(\beta u'')']_\alpha = 0$$

The interface is $\alpha = \frac{\pi}{6}$ and the following configurations of the values for β (x) are considered:

Case 1: $B^- = 2, B^+ = 5$

Case 2: $B^- = 2, B^+ = 500$

Case3: $B^- = 2, B^+ = 50000$

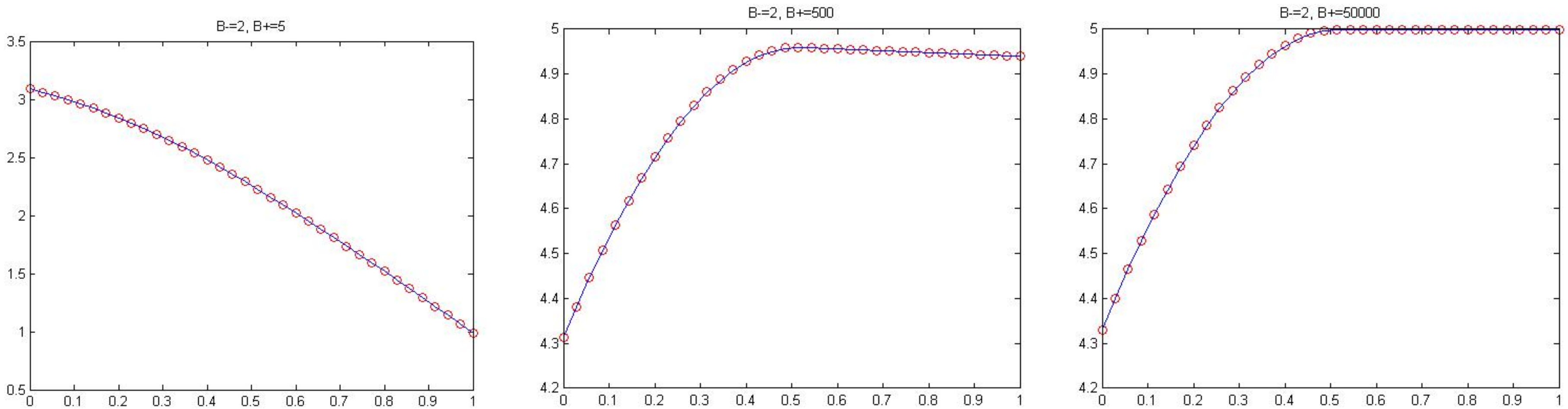
B-=2, B+=5
3.5
3
2.5
2
1.5
1
0.5
0
0.1
0.2
0.3
0.4
0.5
0.6
0.7
0.8
0.9
1
B-=2, B+=500
5
4.9
4.8
4.7
4.6
4.5
4.4
4.3
4.2
B-=2, B+=50000

IFEM for a 2d elliptic problem

$$-\nabla \cdot (\beta \nabla u) = f, \qquad (x,y) \in \Omega$$
$$u \mid_{\partial\Omega} = g,$$
$$[u] \mid_{\tilde{\Gamma}} = 0,$$
$$[\beta u_n] \mid_{\tilde{\Gamma}} = 0.$$

$$\Omega^- = \{(x,y) : x^2 + y^2 \le {r_0}^2\}.$$

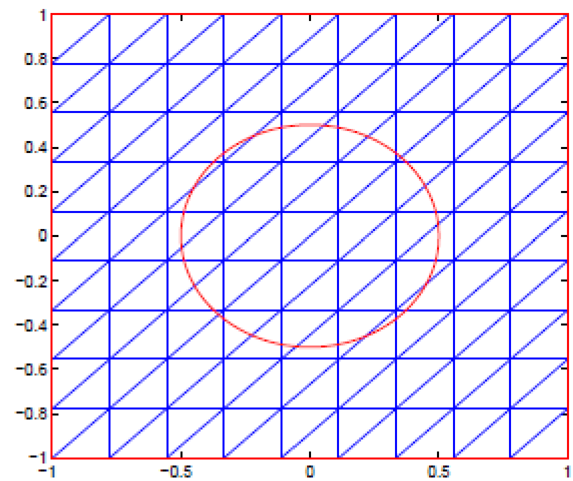

Exact solution:

$$u(x,y) = \begin{cases} \dfrac{r^\alpha}{\beta^-}, & \text{if } r \le r_0, \\ \dfrac{r^\alpha}{\beta^-} + \left(\dfrac{1}{\beta^-} - \dfrac{1}{\beta^+}\right){r_0}^\alpha & \text{otherwise,} \end{cases}$$

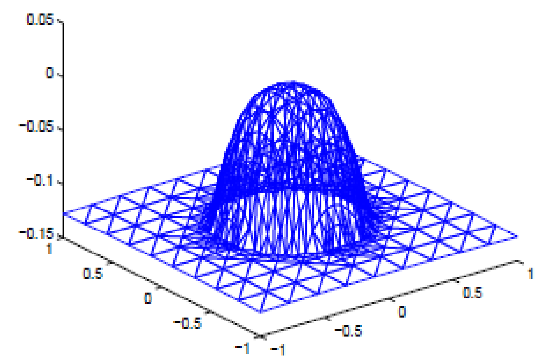

Basis functions

$$\phi^+ = a_0 + a_1 x + a_2 y \text{ for } (x, y) \in T^+$$
$$\phi^- = b_0 + b_1 x + b_2 y \text{ for } (x, y) \in T^-.$$

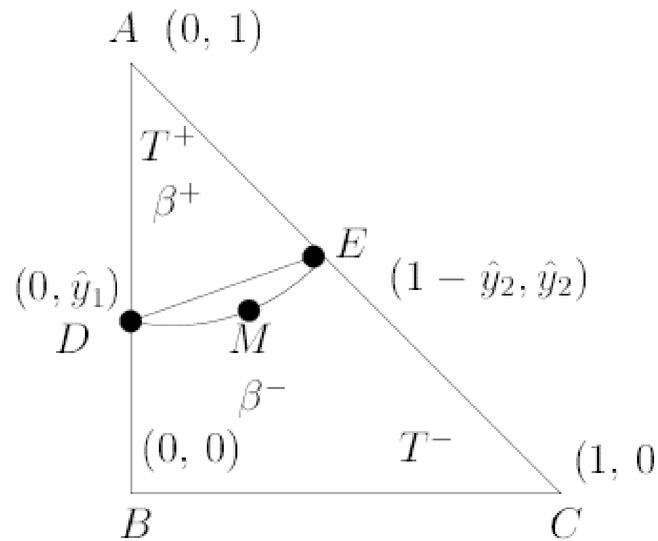

Interface conditions:

$$\phi^+(D) = \phi^-(D)$$

$$\begin{cases} \vec{n}(\Phi^{-1})^T \nabla \phi^+ = \rho \vec{n}(\Phi^{-1})^T \nabla \phi^- \\ \vec{t}(\Phi^{-1})^T \nabla \phi^+ = \vec{t}(\Phi^{-1})^T \nabla \phi^-, \end{cases}$$

To find the basis functions, one only needs to solve a 3x3 linear system:

$$(-1 + \hat{y}_1) a_2 - \hat{y}_1 b_2 = \phi_1 - \phi_3.$$
$$m_1 a_1 + m_2 a_2 - \rho m_2 b_2 = -\rho m_1 \phi_1 + \rho m_1 \phi_2$$
$$m_3 a_1 + m_4 a_2 = m_3(\phi_2 - \phi_1) + m_4 b_2.$$

$$a_0 = \phi_3 - a_2$$
$$b_0 = \phi_1$$
$$b_1 = \phi_2 - \phi_1$$

Error estimation for IFEM

Interpolation error estimation:

Theorem 3.1 *Let T be a triangle in a uniform mesh $\Im_h$ and the interface $\tilde{\Gamma}$ satisfies the hypothesis $(H1)$, $(H2)$ and $(H3)$. Let Γ_T denote the line segment that approximates $\tilde{\Gamma}_T$. Let ϕ be an arbitrary function in $C^2(T)$ and $\phi_I \in S_h^I(T)$ be the IFE interpolant of ϕ. The following error estimates hold.*

$$\|\nabla\phi(x,y) - \nabla\phi_I(x,y)\|_{\infty,T} \leq \begin{cases} ch \left\| D^2\phi \right\|_{\infty,T} & \text{when } (x,y) \in \Omega \backslash T^* \\ c \left\| D^2\phi \right\|_{\infty,T} & \text{when } (x,y) \in T^* \end{cases} \tag{19}$$

$$\|\phi(x,y) - \phi_I(x,y)\|_{\infty,T} \leq ch^2 \left\| D^2\phi \right\|_{\infty,T}, \tag{20}$$

where $c = O(\max\{\frac{1}{\rho}, \rho\})$ and T^* is the region enclosed by $\tilde{\Gamma}_T$ and Γ_T.

Theorem 3.2 *The following interpolation error estimates hold. For function $\phi \in H^2(\Omega)$, if ϕ is a piecewise C^2 function on any interface element τ, for all $\tau \in \mathring{\Im}_h$, then there exist constants c_0 and c_1 such that*

$$\|\phi - \phi_I\|_0 < c_0 h^2 \|\phi\|_2 \tag{39}$$

$$\|\phi - \phi_I\|_1 < c_1 h \|\phi\|_2, \tag{40}$$

where c_0 and c_1 are $O(\max\{1/\rho, \rho\})$.

- A priori error estimation: rigorous proof: one needs the 2nd Strange Lemma. For detail, please see

So-Shiang Chou, Do Y. Kwak and K. T. Wee, Optimal convergence analysis of an immersed interface finite element method, Adv Comput Math, 2009, DOI 10.1007/s10444-009-9122-y.

Theorem 4.8 *Let* $u \in \widetilde{H}^2(\Omega)$, $\hat{u}_h \in \widehat{S}_h(\Omega)$ *be the solutions of* (2.3) *and* (4.1) *respectively. Then there exists a constant* $C > 0$ *such that*

$$\|u - \hat{u}_h\|_{1,h} \leq Ch\|u\|_{\widetilde{H}^2(\Omega)}. \tag{4.20}$$

Theorem 5.1 *Let* $u \in \widetilde{H}^2(\Omega)$, $\hat{u}_h \in \widehat{S}_h(\Omega)$ *be the solutions of* (2.3) *and* (4.1) *respectively. Then there exists a constant* $C > 0$ *such that*

$$\|u - \hat{u}_h\|_{L^2(\Omega)} \leq Ch^2\|u\|_{\widetilde{H}^2(\Omega)}. \tag{5.4}$$

Numerical tests for 2nd order elliptic interface problem:

A priori error check:

h	$\frac{\beta_1^-}{\beta_1^+} = 10^{-1}$	$\frac{\beta_2^-}{\beta_2^+} = 10^{-2}$	$\frac{\beta_3^-}{\beta_3^+} = 10^{-3}$
$\frac{1}{8}$	3.689e-03	3.676e-03	4.164e-03
$\frac{1}{16}$	9.897e-04	9.998e-04	1.110e-03
$\frac{1}{32}$	2.700e-04	2.673e-04	3.370e-04
$\frac{1}{64}$	6.766e-05	6.318e-05	7.567e-05

Error in L2 norm

h	$\frac{\beta_1^-}{\beta_1^+} = 10^{-1}$	$\frac{\beta_2^-}{\beta_2^+} = 10^{-2}$	$\frac{\beta_3^-}{\beta_3^+} = 10^{-3}$
$\frac{1}{8}$	1.922e-01	4.677e-01	1.471e-00
$\frac{1}{16}$	8.314e-02	1.439e-01	4.390e-01
$\frac{1}{32}$	4.526e-02	8.726e-02	2.686e-01
$\frac{1}{64}$	2.222e-02	2.942e-02	8.394e-02

Error in H1 norm

Linear regression shows that :

$$\left\|u - u_h^I\right\|_0 \approx 0.25h^{1.97},\ \left\|u - u_h^I\right\|_0 \approx 0.27h^{2.00} \text{ and, } \left\|u - u_h^I\right\|_0 \approx 0.28h^{1.96},$$

$$\left\|u - u_h^I\right\|_{\beta_1} \approx 1.71h^{1.05},\ \left\|u - u_h^I\right\|_{\beta_2} \approx 6.89h^{1.30},\ \text{and } \left\|u - u_h^I\right\|_{\beta_3} \approx 6.75h^{1.00}.$$

- A posteriori estimation: We follow Verfurth's frame works.

$$\left\|u - u_h^I\right\|_\beta \leq c_p\{\sum[\eta_\tau^2 + h_\tau^2\beta_\tau^{-1}\left\|f - f_\tau\right\|_{0,\tau}]\}^{\frac{1}{2}},$$

$$\eta_\tau = \left\{h_\tau^2\beta_\tau^{-1}\left\|f_h + div\beta_\tau\nabla u_h^I\right\|_{0,\tau}^2 + \frac{1}{2}\sum_{e\in\partial\tau} h_e\beta_\tau^{-1}\left\|\beta_\tau\left[\partial_{n_e}u_h^I\right]\right\|_{0,e}^2\right\}^{\frac{1}{2}},$$

$$\eta_\tau = \left\{\max\{\rho, \frac{1}{\rho}\}\left(\sum_{\tau'\in\{\tau^+,\tau^-\}} h_{\tau'}^2\beta_{\tau'}^{-1}\left\|f_h + div\beta_{\tau'}\nabla u_h^I\right\|_{0,\tau'}^2 + \frac{1}{2}\sum_{e'\in\{\partial^+\tau,\partial^-\tau\}} h_{e'}\beta_{e'}^{-1}\left\|\beta_{e'}\left[\partial_{n_{e'}}u_h^I\right]\right\|_{0,e'}^2\right)\right\}^{\frac{1}{2}},$$

R. Verfürth. *A review of posteriori error estimation and adaptive mesh-refinement techniques.* 1996.

C. Bernardi and R. Verfürth. Adaptive finite element methods for elliptic equations with non-smooth coefficients. *Numer. Math.*, 85:579–608, 2000.

A posteriori error check:

$\beta^- = 1, \beta^+ = 10$

$\lvert N_h \rvert$	$\lVert u - u_h^I \rVert_\beta$	$\left(\sum_{\tau \in \Im_h} \eta_\tau^2\right)^{1/2}$
324	1.922e-01	4.117e-00
557	1.338e-01	2.316e-00
899	1.217e-01	1.756e-00
2516	6.281e-02	1.054e-00
3527	6.116e-02	7.515e-01
10482	3.097e-02	3.842e-01

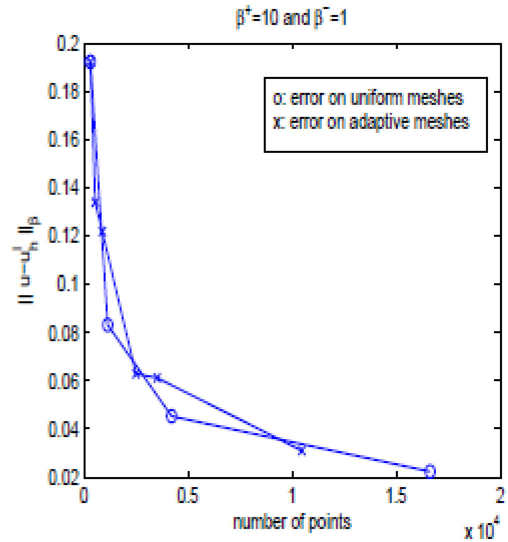

$\beta^- = 1, \beta^+ = 100$

$\lvert N_h \rvert$	$\lVert u - u_h^I \rVert_\beta$	$\left(\sum_{\tau \in \Im_h} \eta_\tau^2\right)^{1/2}$
324	4.677e-01	1.136e+01
466	1.958e-01	1.538e+01
682	1.341e-01	2.280e-00
1507	5.495e-02	1.088e-00
4171	3.139e-02	5.201e-01
10243	2.188e-02	3.134e-01

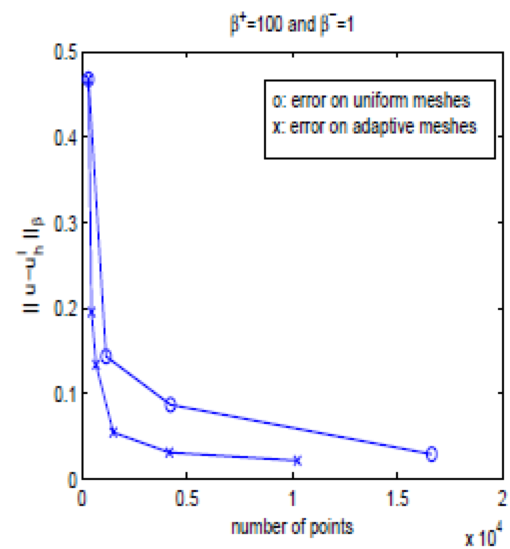

$$\beta^- = 1, \beta^+ = 1000$$

$\lvert N_h \rvert$	$\lVert u - u_h^I \rVert_\beta$	$\left(\sum_{\tau \in \Im_h} \eta_\tau^2\right)^{1/2}$
324	1.471e-00	1.592e+02
410	6.378e-01	1.659e+02
626	5.332e-01	8.339e-00
1066	2.057e-01	3.673e-00
1923	1.251e-01	1.572e-00
4021	4.105e-02	6.986e-01

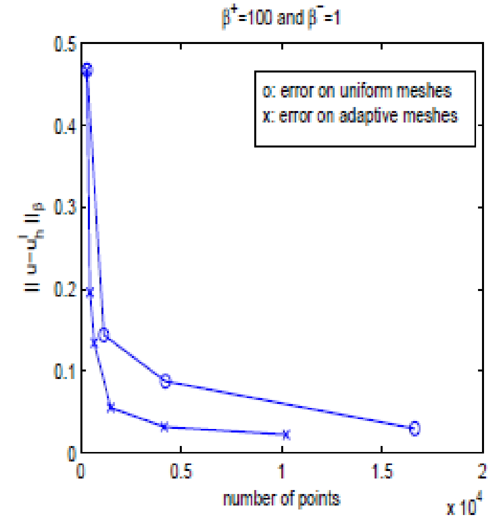

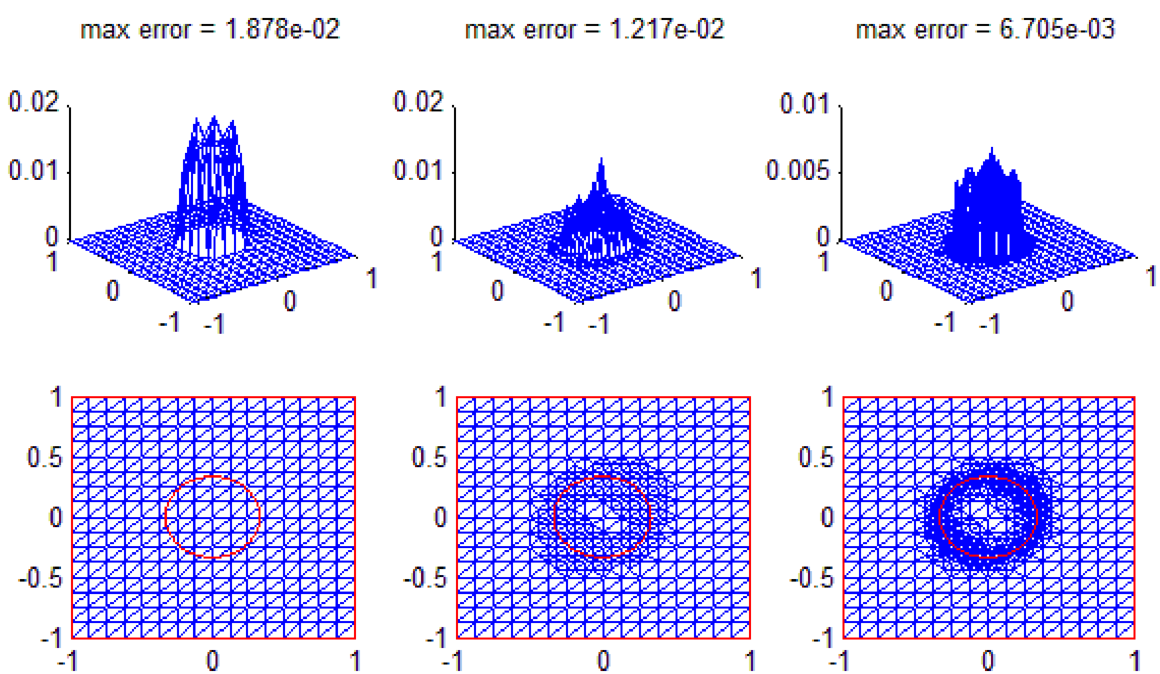

IFEM for a 2d elastic system

$$\int_{\Omega} \begin{pmatrix} \partial_1 v_1 \\ \partial_2 v_2 \\ \partial_2 v_1 + \partial_1 v_2 \end{pmatrix}^T \begin{pmatrix} \lambda + 2\mu & \lambda & 0 \\ \lambda & \lambda + 2\mu & 0 \\ 0 & 0 & \mu \end{pmatrix} \begin{pmatrix} \partial_1 u_1 \\ \partial_2 u_2 \\ \partial_2 u_1 + \partial_1 u_2 \end{pmatrix} dx$$

$$- \int_{\partial\Omega} v_1 \left(\lambda \nabla \cdot u + 2\mu \partial_1 u_1, \mu \left(\partial_2 u_1 + \partial_1 u_2 \right) \right) \cdot \mathbf{n} \, ds$$

$$- \int_{\partial\Omega} v_2 \left(\mu \left(\partial_2 u_1 + \partial_1 u_2 \right), \lambda \nabla \cdot u + 2\mu \partial_2 u_2 \right) \cdot \mathbf{n} \, ds = 0$$

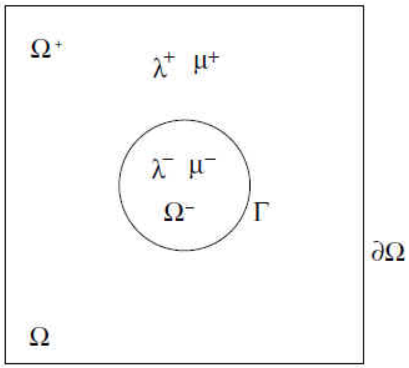

Figure 1: A rectangular domain Ω with an immersed interface Γ.

Interface conditions:

$$\left[\lambda \left(\frac{\partial u_1}{\partial x_1} + \frac{\partial u_2}{\partial x_2} \right) n_1 + 2\mu \frac{\partial u_1}{\partial x_1} n_1 + \mu \left(\frac{\partial u_1}{\partial x_2} + \frac{\partial u_2}{\partial x_1} \right) n_2 \right]_\Gamma = q_1,$$

$$\left[\lambda \left(\frac{\partial u_1}{\partial x_1} + \frac{\partial u_2}{\partial x_2} \right) n_2 + 2\mu \frac{\partial u_2}{\partial x_2} n_2 + \mu \left(\frac{\partial u_1}{\partial x_2} + \frac{\partial u_2}{\partial x_1} \right) n_1 \right]_\Gamma = q_2,$$

Flux-jump conditions

$$[u_1]_\Gamma = w_1, \ \ [u_2]_\Gamma = w_2.$$

Interface continuity conditions

Assume basis functions ϕ and ψ of the displacement vector $\left(u_1, u_2\right)$ are both linear in T^- and T^+ of the interface element T

There are total 12 coefficients of these basis functions to be determined! By solving the linear system given by

- 6 nodal continuity constrains
- 4 interface continuity constrains
- 2 interface jump conditions

One can construct the basis functions of the interface element!

Theorems, implementation and numerical results can be seen in Yan Gong's PhD thesis 2007 (Thesis advisor: Zhilin Li)

We are working on IFEM for bi-harmonic equation in 2D for the PZT composite diaphragm and the fluid-structure Interface.

Intrusion detection problem

EIT (Electrical Impedance Tomography)

Different materials have different electric conductivity σ and permittivity ε

tissue	$1/\sigma$ (Ohm-cm)	ϵ (μF/m)
lung	950	0.22
muscle	760	0.49
liver	685	0.49
heart	600	0.88
fat	> 1000	0.18

Table 1: Electrical properties of biological tissue measured at frequency 10kHz [10, 131]

rock or fluid	$1/\sigma$ (Ohm-cm)
marine sand, shale	1 - 10
terrestrial sands, claystone	15 - 50
volcanic rocks, basalt	10 - 200
granite	500 - 2000
limestone dolomite, anhydrite	50 - 5000
chloride water from oil fields	0.16
sulfate water from oil fields	1.2

Table 2: Resistivity of rocks and fluids [99]

EIT is the inverse problem of determining the impedance in the interior of a domain, given simultaneous measurements of the direct or alternating electric currents and voltages at the boundary of the domain

Some good introductions can be found in

1. M. Cheney, D. Isaacson and J. C. Newell, Electrical Impedance Tomography. SIAM review, Vol 41, No. 1. pp. 85-101.

2. Liliana Borcea, http://www.caam.rice.edu/~borcea/Lectures/index.html

Mathematical Model

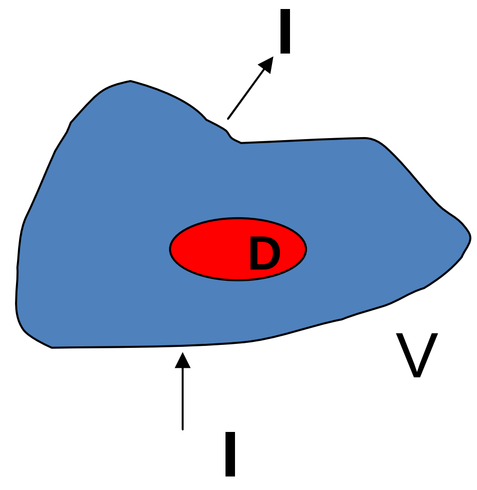

$$(*) \quad \begin{cases} \nabla \cdot \left[\gamma(x,\omega) \nabla \phi(x,\omega) \right] = 0 \text{ in } \Omega \\ \phi(x,\omega) = V(x,\omega) \text{ on } \partial\Omega \end{cases}$$

here ϕ is the electrical potential and $\gamma(x,\omega)$ is the admittivity.

Q: How to reconstruct $\gamma(x,\omega)$ by measuring the current $I = \dfrac{\partial \phi}{\partial n}$?

Maxwell Equation:

$\nabla \times \mathrm{E}(\mathrm{x},\omega) = -i\omega\mu(x)H(x,\omega)$, here μ is the magnetic permeability

$\omega\mu[\sigma][x]^2 \ll 1$ (typical parameter
ω=28.8 KHZ, $[\sigma] \le 1$, and $[x] \le 1$)

$$E = -\nabla\phi(x,\omega)$$

$$\nabla \times H(\mathrm{x},\omega) = \left[\sigma(x) + i\omega\varepsilon(x)\right]E(x,\omega)$$

$$\nabla \cdot \left(\nabla \times H(\mathrm{x},\omega)\right) = \nabla\left(-\gamma\nabla\phi(x,\omega)\right) = 0$$

Apply current J_b on the boundary

$$\nabla \cdot \left(-\gamma\nabla\phi\right) = 0 \Rightarrow \int_{\partial\Omega} \gamma \frac{\partial\phi}{\partial n}\,\mathrm{ds} = \int_{\partial\Omega} J_b \, ds$$

Theorems

Theorem 1

Consider $U_{N,t,h} = \chi_{N,t} e^{\frac{-1/t}{h}} U_{N,h}$ here $U_{N,h} = e^{C_N X^N}$, $X^N = \varphi(x) + \mathrm{i}\,\psi(x)$ is a complex conformal mapping (the complex geometrical optical solution), and $\chi_{N,t}$ is the cut off function on the conic region contains level curves of $\varphi(x) = \frac{1}{\mathrm{t}}$.

Consider $W_{N,t,h}$ be the solution of $(*)$ with Dirichlet data $U_{N,t,h}$ on $\partial\Omega$. There exists constants c and ε such that

$$\left\| U_{N,t,h} - W_{N,t,h} \right\|_2 < c e^{-\frac{\varepsilon}{h}} \ for\ h \ll 1.$$

Probing Level Curves

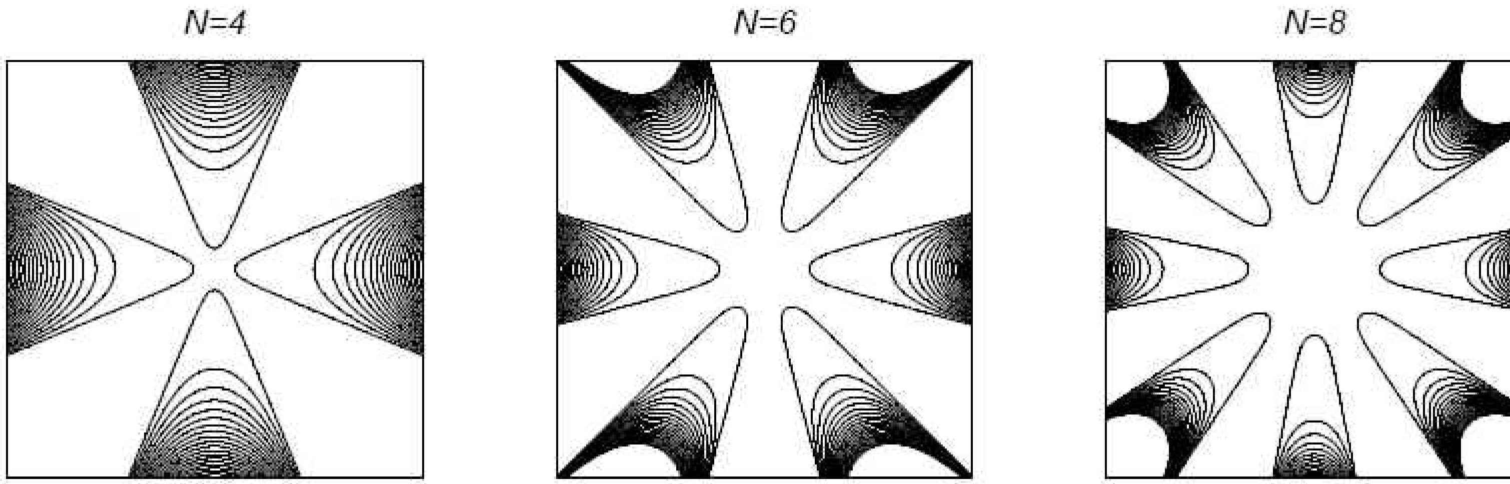

FIGURE 4.1. Some level curves of ϕ_N.

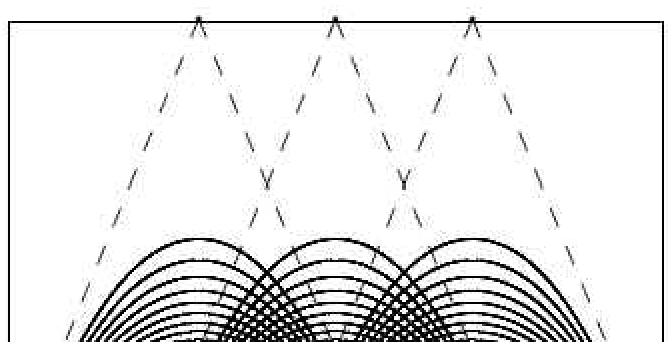

A probing sequence

Theorem 2

Assume for any $\mathrm{p} \in \partial \mathrm{D}$, there exist $\mathrm{B}_{\varepsilon}(p)$ such that

$\delta\gamma > \varepsilon,$ here $\delta\gamma = \gamma_D - \gamma_\Omega > 0$ and $\gamma = \gamma_\Omega + \chi_{\mathrm{D}}\delta\gamma$.

Let $\Lambda_0 : V \rightarrow \gamma_\Omega \dfrac{\partial \phi}{\partial n}$ be the associated (DtN map) without instrusion and

$\Lambda_{\mathrm{D}} : V \rightarrow \gamma \dfrac{\partial \phi}{\partial n}$ be the DtN map with instrusion D.

The following inequalities hold.

$$\int_{\partial\Omega} (\Lambda_{\mathrm{D}} - \Lambda_0)\overline{V} \cdot V \; ds \le \int_D \delta\gamma \left|\nabla \phi\right|^2 dx$$

$$\int_{\partial\Omega} (\Lambda_{\mathrm{D}} - \Lambda_0)\overline{V} \cdot V \; ds \ge \int_D \frac{\gamma_\Omega \delta\gamma}{\gamma_D} \left|\nabla \phi\right|^2 dx$$

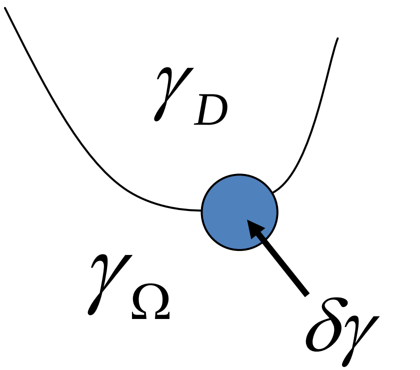

Theorem 3

Let ℓ_{t} be the level curve of $\varphi(x) = \dfrac{1}{\mathrm{t}}$ and

$\mathrm{E}(N,t,h) = \int_{\partial\Omega} (\Lambda_{\mathrm{D}} - \Lambda_0)\overline{V}_{N,t,h} \cdot V_{N,t,h}\, ds$. We have

(i) if $\ell_{\mathrm{t}} \cap \overline{D} = \phi,$ then $\exists\ \varepsilon_1$ and h_1, $\mathrm{E}(N,t,h) \prec e^{-\varepsilon_1/h}$ for all $\mathrm{h} \geq \mathrm{h}_1$

(ii) if $\ell_{\mathrm{t}} \cap \overline{D} \neq \phi,$ then $\exists\ \varepsilon_2$ and h_2, $\mathrm{E}(N,t,h) \succ e^{-\varepsilon_2/h}$ for all $\mathrm{h} \geq \mathrm{h}_2$

Remarks:

1. **The constant c in Theorem 1 depends on the phase angle of the CGO solution. The estimations in Theorem 1 and 3 are sharp only for small phase angles.**

Numerical results

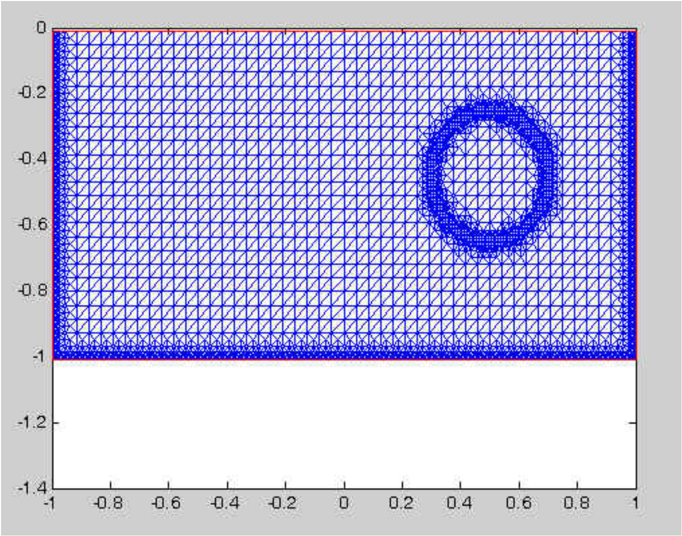

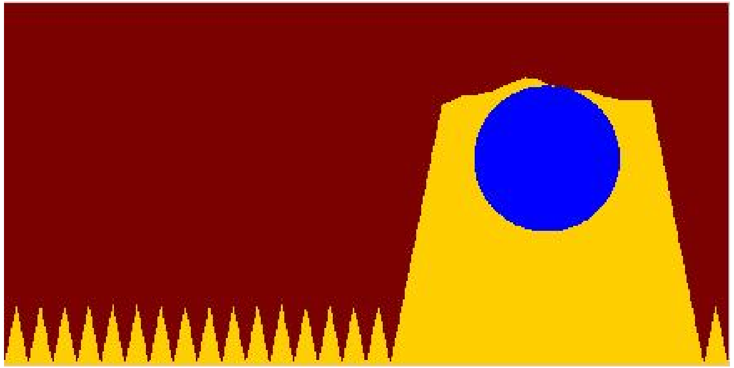

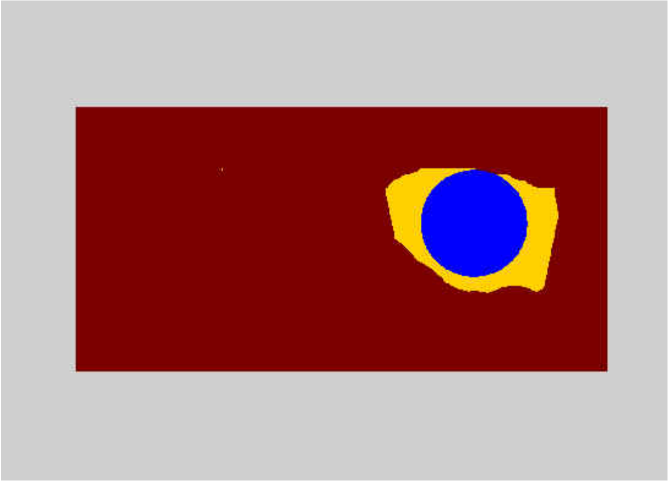

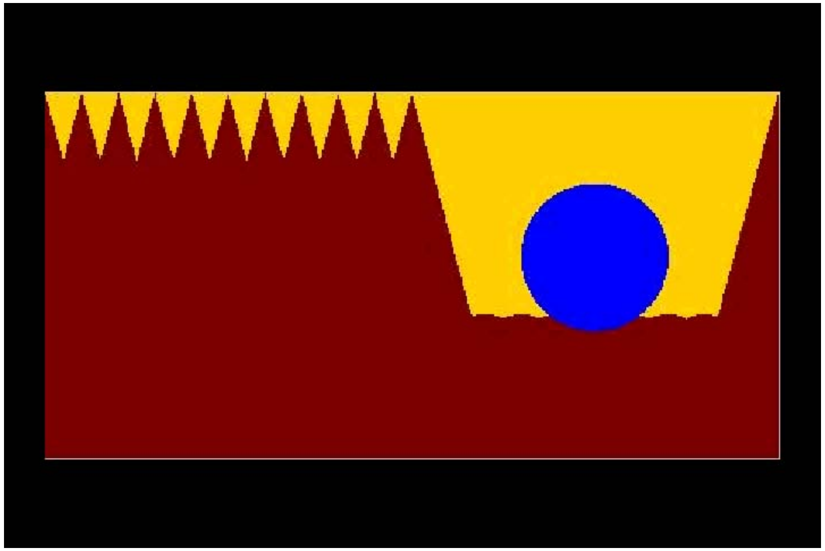

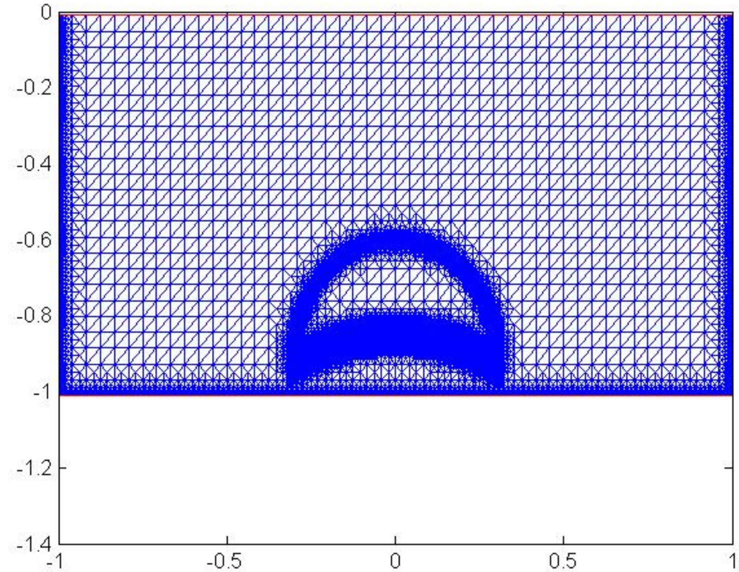

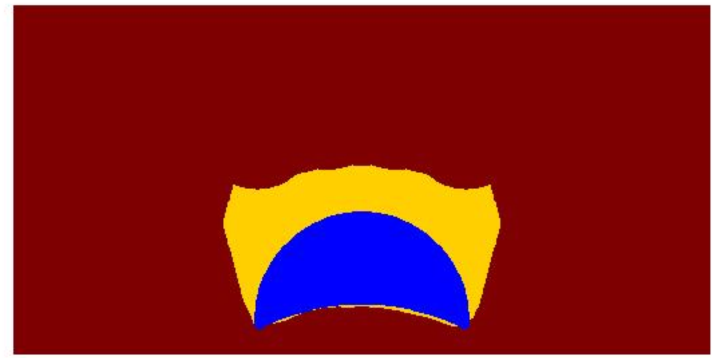

reconstruction

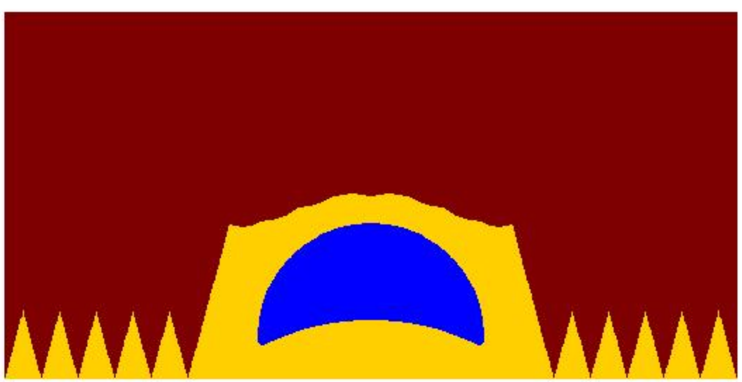

reconstruction

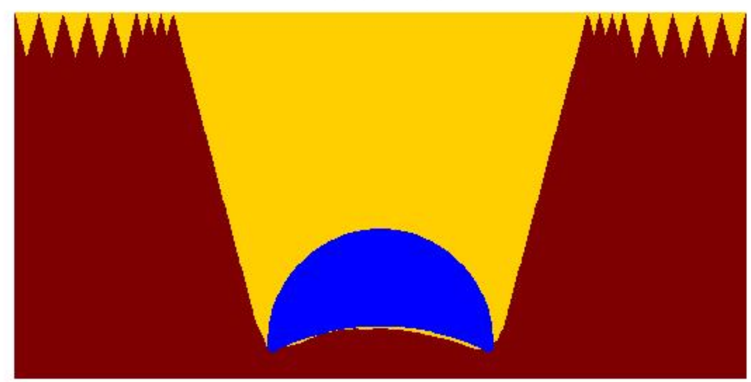

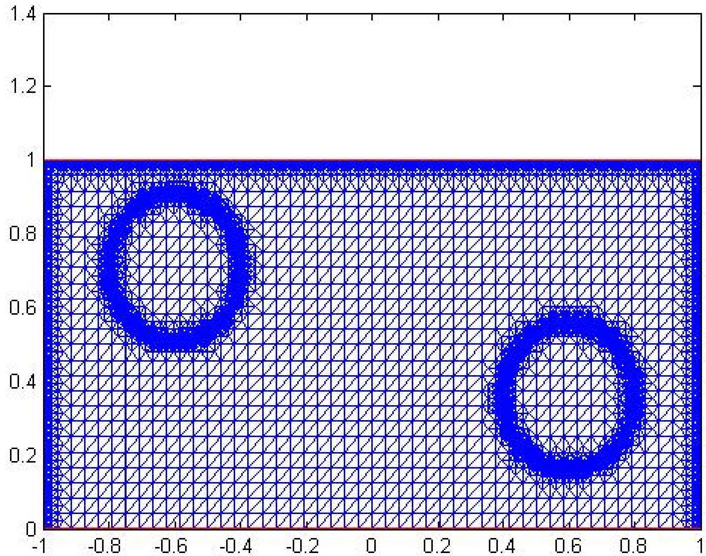
1.4
1.2
1
0.8
0.6
0.4
0.2
0
-1
-0.8
-0.6
-0.4
-0.2
0
0.2
0.4
0.6
0.8
1

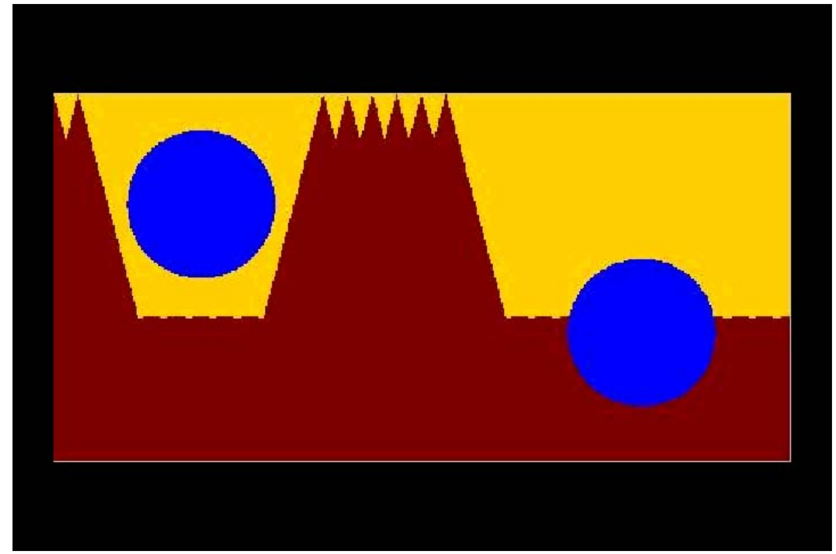

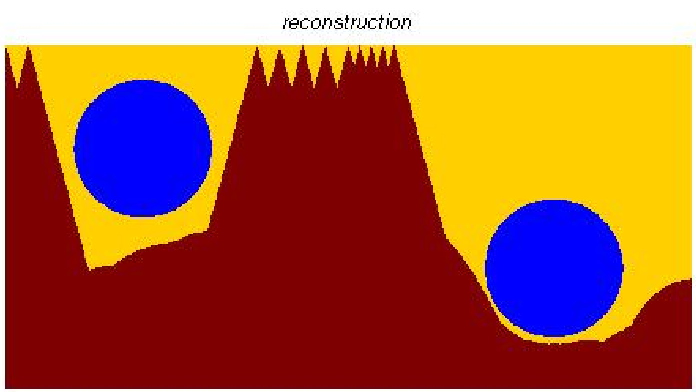
reconstruction

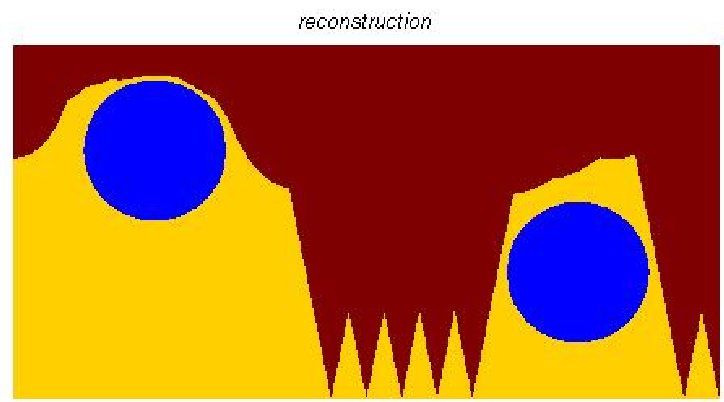
reconstruction

Reconstruction in Elastic System

Mathematical Model:

$$\begin{cases} \nabla \cdot \left(\left(\lambda \nabla u \right) I + 2\mu S\left(\nabla u \right) \right) = 0 \\ u\big|_{\partial\Omega} = g \end{cases},$$

here $\mathrm{S}\left(\mathrm{A}\right) = \dfrac{A + A^T}{2}$ and $\sigma\left(u\right) = \left(\lambda \nabla u\right) I + 2\mu S\left(\nabla u\right)$

is the stress tensor

DtN map: $$\Lambda_{\mathrm{D}} : g \to \sigma\left(u\right) \cdot \vec{n}$$

Energy quantity:

$$\mathrm{E}\left(N, t, h\right) = \int_{\partial\Omega} \left(\Lambda_{\mathrm{D}} - \Lambda_0\right) \overline{g}_{N,t,h} \cdot g_{N,t,h} \, ds.$$

Through direct computing, the weak form of the system PDE can be rewritten as

$$\int_\Omega \begin{bmatrix} \frac{\partial v_1}{\partial \mathrm{x}} & \frac{\partial v_2}{\partial y} & \frac{\partial v_1}{\partial \mathrm{x}}+\frac{\partial v_2}{\partial y} \end{bmatrix} C \begin{bmatrix} \frac{\partial u_1}{\partial \mathrm{x}} & \frac{\partial u_2}{\partial y} & \frac{\partial u_1}{\partial \mathrm{x}}+\frac{\partial u_2}{\partial y} \end{bmatrix}^T dx -$$

$$\int_{\partial\Omega} \begin{bmatrix} v_1 & v_2 \end{bmatrix} \begin{bmatrix} \lambda\nabla\cdot u+2\mu\frac{\partial u_1}{\partial \mathrm{x}} & \mu\left(\frac{\partial u_1}{\partial y}+\frac{\partial u_2}{\partial \mathrm{x}}\right) \\ \mu\left(\frac{\partial u_1}{\partial y}+\frac{\partial u_2}{\partial \mathrm{x}}\right) & \lambda\nabla\cdot u+2\mu\frac{\partial u_2}{\partial y} \end{bmatrix} \cdot \vec{n}\; ds, \quad \text{here,}$$

$$\mathrm{C}=\begin{bmatrix} \lambda+2\mu & \lambda & 0 \\ \lambda & \lambda+2\mu & 0 \\ 0 & 0 & \mu \end{bmatrix}$$ is the stress-strain relationship

and, $\lambda\nabla\cdot u+2\mu\frac{\partial u_1}{\partial \mathrm{x}}$ and $\mu\left(\frac{\partial u_1}{\partial y}+\frac{\partial u_2}{\partial \mathrm{x}}\right)$ are the normal stress and shear stress.

Numerical Studies

Consider λ and μ are constant, here $\lambda = \frac{\mathrm{E}\nu}{(1+\mathrm{v})(1\text{-}2\nu)}, \mu = \frac{E}{2(1+\nu)}$

where $(\mathrm{E},\nu) = \begin{cases} (6\times10^6, 0.45) \text{ in } \Omega\backslash\mathrm{D} \\ (6\times10^7, 0.45) \text{ in } \mathrm{D} \end{cases}$

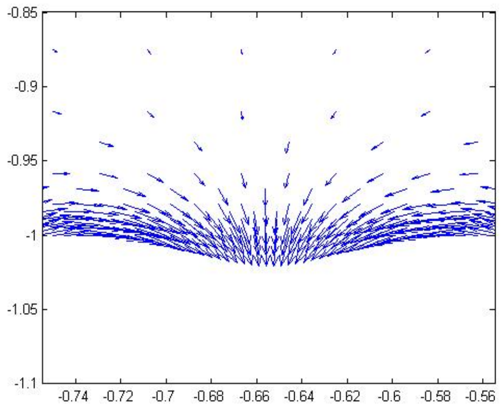

The special solution can be given by

$$u_{N,t,h} = \chi_{N,t} e^{\frac{-1/t}{h}} U_{N,h}$$

here $U_{N,h} = e^{C_N X^N} \nabla X^N, X^N = \varphi(x) + \mathrm{i}\psi(x)$

Displacement field near the boundary

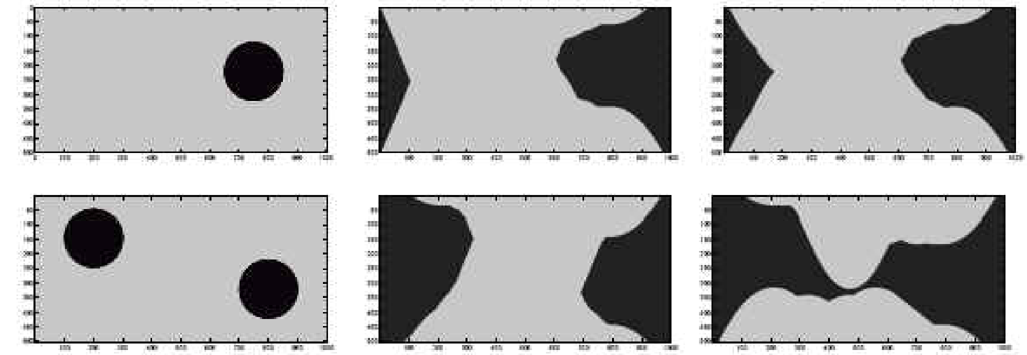

FIGURE 4.3. The first column represents the actual location of the inclusion. The second column is the numerical reconstruction with noiseless simulated data. The third column is the numerical reconstruction with noisy data with $A = 0.01\%$. All gray areas are inclusion-free

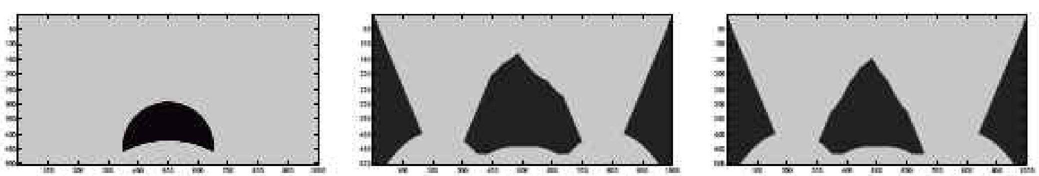

FIGURE 4.5. The first column is the actual location of the inclusion. The second column is the numerical reconstruction with noiseless simulated data when Ω is a rectangle. The third column is the numerical reconstruction with noiseless simulated data when Ω is a strip. All gray areas are inclusion-free regions.

Conclusion

More works to be done!!!

- Immersed finite element method for PZT Interface and fluid-structure interface
- Accurate elliptic solver on evolving surface
- Intrusion and crack detection for PZT
- Fracture and fatigue analysis of PZT membrane
- Resonance of fluid and composite structure

Thanks for your attention